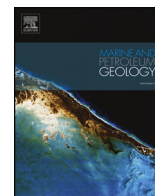




ELSEVIER

Contents lists available at ScienceDirect

Marine and Petroleum Geology

journal homepage: www.elsevier.com/locate/marpetgeo

Research paper

Origin of fluids discharged from mud volcanoes in SE Iran

Mahin Farhadian Babadi^{a,*}, Behzad Mehrabi^a, Franco Tassi^{b,c}, Jacopo Cabassi^{b,c},
Orlando Vaselli^{b,c}, Ata Shakeri^a, Elena Pecchioni^b, Stefania Venturi^b, Michael Zelenski^d,
Ilya Chaplygin^e

^a Department of Geochemistry, Faculty of Earth Sciences, Kharazmi University, Tehran, Iran^b Department of Earth Sciences, University of Florence, Via G. La Pira 4, 50121 Florence, Italy^c CNR-IGG Institute of Geosciences & Earth Resources, Via G. La Pira 4, 50121 Florence, Italy^d Institute of Experimental Mineralogy, Russian Academy of Science, Russia^e Institute of Geology of Ore Deposits, Petrology, Mineralogy and Geochemistry, Russian Academy of Science, Russia

ARTICLE INFO

Keywords:

Mud volcanoes
Iran
Thermogenic hydrocarbons
Water-rock interactions
Hydrothermal fluids

ABSTRACT

Onshore and offshore mud volcanism in the Makran accretionary prism is related to convergence of the Arabian and Eurasian plates. This study describes the chemical and isotopic composition of hydrocarbon-rich fluids from four active on-shore mud volcanoes located along the Makran coast (southern Iran), namely Borborok, Ain, Napag and Sand Mirsuban (Makran coast, southern Iran), as well as Pirlgel mud volcano (SE Iran) that is located between the Taftan and Bazman igneous volcanoes. The main aim was to provide insights into the source region (s) of gases and waters discharged from these systems and the secondary processes controlling their chemical features. The four on-shore mud volcanoes emitted CH₄-dominated gases, with significant concentrations of C₂₊ alkanes suggesting a dominant thermogenic origin, as confirmed by their δ¹³C–CH₄ values. Carbon dioxide was present at relatively low concentrations (0.78–2.33%) with an isotopic signature (δ¹³C–CO₂ from –34.2 to –11.1‰ vs. V-PDB) in the range of that typical of thermogenic gases. Hence, the geochemical features of these mud volcanoes point to the occurrence of a deep gas source rich in hydrocarbons, although the occurrence of an exploitable gas reservoir has to be confirmed by geophysical measurements and detailed geostructural surveys. Gas chemistry from Pirlgel mud volcano completely differs with respect to that of the previous ones, since the former emits gases dominated by CO₂ and showing relatively high R/Ra values (≈ 1.6), suggesting a significant fluid contribution from the nearby volcanic systems. Moreover, waters from the on-shore mud volcanoes showed a Na–Cl composition, typically associated with mud volcanism, whereas those discharged from Pirlgel were Na–HCO₃-type and rich in chemical species typical of hydrothermal fluids such as As. Waters from the on-shore volcanoes were characterized by a strong δ¹⁸O-positive shift and high B and Li concentrations, likely indicating clay mineral dehydration and long-term water-rock interaction. Such geochemical features were also shown by the waters from Pirlgel, where the high concentrations of B and Li were possibly related to volcanic source. Estimated temperatures for the on-shore mud volcanoes estimated using the Mg–Li and Mg–K geothermometers range from 84 to 165 °C, corresponding to 3–7 km depth.

1. Introduction

Mud volcanoes are commonly recognized in subaerial and submarine environments as a result of extrusion of subsurface pressurized fluids, argillaceous material, petroleum products and clasts. Organic gas compounds associated with mud volcanism are typically dominated by CH₄ (Dia et al., 1999; Dimitrov, 2002; Etiopie et al., 2004; Milkov et al., 2003), with significant concentrations of heavier hydrocarbons, CO₂, H₂S, N₂ and noble gases (Blinova et al., 2003; Tassi et al., 2012). Mud

volcanoes emitting CO₂-rich fluids were occasionally recognized close to volcanic areas (Chiodini et al., 1996; Giammanco et al., 2007; Shakirov et al., 2004; Tassi et al., 2012; Yang et al., 2004).

In submarine environments, mud volcanism commonly produces gas hydrates and CH₄-derived authigenic carbonates, whose origin is typically related to CH₄ oxidation and activity of methanotrophic archaea and sulfate reducing bacteria (e.g. Himmeler et al., 2015; Liang et al., 2016; Naehr et al., 2007). These geological structures frequently occur along the Alpine-Himalayan collision zone, on accretionary

* Corresponding author.

E-mail address: mahin.farhadian@khu.ac.ir (M. Farhadian Babadi).<https://doi.org/10.1016/j.marpetgeo.2019.05.005>

Received 13 February 2019; Received in revised form 2 May 2019; Accepted 6 May 2019

Available online 11 May 2019

0264-8172/ © 2019 Elsevier Ltd. All rights reserved.

complexes (e.g. Gulf of Cadiz, Mediterranean Ridge and Makran) and forelands (e.g. Northern Apennines, Romania, Kerch and Taman peninsulas, and Azerbaijan), as well as in dipping non-compensating sedimentary basins associated with active plate boundaries (Black Sea and South Caspian basins) (Dimitrov, 2002). Mechanisms of mud volcano formation were mostly investigated in the framework of hydrocarbon exploration (e.g. Dimitrov, 2002; Kopf, 2002; Prinzhofer and Deville, 2013; Wan et al., 2013). The presence of mud volcanoes is usually interpreted as a clear indication of tectonically active zones, where sediments are affected by compressive stress causing (i) pressurization of fluids and/or buoyancy forces due to density inversion and (ii) formation of surface-piercing shale diapirs, as well as narrow zones of weakness (e.g. faults and fractures) or anticlines (Brown, 1990; Deville et al., 2006; Dimitrov, 2002; Kopf et al., 2001; Kopf, 2002; Milkov, 2000). As a rule, light alkanes (C₁–C₄) produced through thermogenic or microbial processes can be distinguished based on C₁/(C₂₊) ratios and their stable carbon ($\delta^{13}\text{C}$) and hydrogen (δD) isotopic values of CH₄ (Bernard et al., 1978; Schoell, 1980, 1988; Whiticar, 1999). A data-set including composition of light alkanes and isotopic values of CH₄ from 143 on-shore mud volcanoes indicated that ~76% of them released thermogenic organic volatiles, whereas the rest emitted either pure microbial CH₄ or gases produced by mixing of the two end members (Etiope et al., 2009). In general, the occurrence of thermogenic hydrocarbons in fluids discharged from mud volcanoes implies that the main organic gas source consists of a deep hydrocarbon reservoir (Milkov, 2005). The chemical and isotopic composition of waters and solids discharged from mud volcanoes may provide further insights into the physical-chemical processes occurring during the underground fluid circulation, such as mineral-water interaction, aquifer mixing, carbonate precipitation and dissolution and clay mineral dehydration (Colten-Bradley, 1987; Dia et al., 1999; Kopf and Deyhle, 2002; Lavrushin et al., 2005; Mazzini et al., 2017; Oppo et al., 2014; Rittenhouse, 1967; You et al. 1993, 1996).

Makran accretionary prism hosts numerous subaerial and submarine sedimentary mud volcanoes. In this area, geochemical and petrological investigations of off-shore mud volcanism revealed the occurrence of huge CH₄ reservoirs (Grando and McClay, 2007; Himmler et al., 2015; Sain et al., 2000; Schlüter et al., 2002). Delisle et al. (2002) reported geochemical data of gases discharged from two on-shore mud volcanoes located along the Makran coast in Pakistan. Conversely, to the best of our knowledge, no geochemical investigations were reported on mud volcanoes in the Iranian side of this region, along the Makran coast in the Sistan and Balochistan Province (Fig. 1A).

In this study, water and gas chemistry, as well as the mineralogical composition of muds discharged from Borborok, Ain, Napag and Sand Mirsuban on-shore mud volcanoes situated in Coastal Makran (Figs. 1A and 2), and Pirlgel mud volcano, located between Taftan and Bazman volcanoes (Figs. 1A and 3), were investigated. The main aims were to (i) provide insights on the geochemical processes affecting the discharged fluids and (ii) obtain information about the hydrocarbon potential from the Coastal Makran area and the west side of Sistan suture zone, since no drilling activity for petroleum exploration were so far carried out.

2. Geological setting

Makran is regarded as one of the largest accretionary wedges on Earth, formed by northward subduction of the Arabian oceanic plate beneath the Eurasian plate, a process that has been active since the late Cretaceous. This area (~900 × 350 km) is delimited to the west by the Minab fault in Iran and to the east by the Ornach-Nal fault in Pakistan. Its prosecution to the south consists of an off-shore front of deformation in the Oman Gulf. The northern limit of the Makran zone is associated with the depressions of Jaz Murian (Iran) and Mashkel (Pakistan) (Platt et al., 1985) (Fig. 1A).

The stratigraphic sequence of the gently sloping Makran subduction

zone includes ~4 km of late Oligocene to middle Miocene Himalayan turbidites, which are unconformably overlaid by 3 km of late Miocene to middle Pleistocene shelf-and-slope sands (Makran sands, Fig. 1B). The Himalayan turbidites, likely deriving from the Indus fan to the east (Kopp et al., 2000), were interpreted as the main décollement of the Makran accretionary wedge (Fig. 1B) (Fowler et al., 1985; Harms et al., 1984; Kopp et al., 2000). These sequences are regarded as the main source for mud volcanism in the area (Delisle et al., 2002; Grando and McClay, 2007; McCall, 2002), which originated from dewatering and consolidation of the subducted sediments related to lateral tectonic compression causing squeezing of fluidized mud along the basal décollement (Fowler et al., 1985; Schlüter et al., 2002). The Iranian Makran accretionary wedge is considered aseismic (Hosseini-Barzai and Talbot, 2003). However, seismicity increased in the Makran mud volcanoes after the Bam earthquake (Mw 6.6; epicenter at 400 km from Makran coast) that occurred on the 26th of December 2003 (Saket et al., 2005). Similarly, the 16 April 2013 eruption of the Napag mud volcano may be related to the Saravan earthquake, which occurred on the same day (Mw 7.8) and whose epicenter was at a distance of ~350 km (Miri et al., 2014).

Iranian Makran consists of four main provinces including, from the North to the South: North, Inner, Outer and Coastal Makran. These provinces are separated by E-W striking thrust faults, reflecting different stages of accretionary wedge evolution (Fig. 1A; Dolati, 2010; Haghypour, 2013). North Makran is dominated by mafic to intermediate Upper Cretaceous to Eocene igneous rocks and tectonic mélanges, whereas Inner Makran consists of Eocene to Lower Miocene terrigenous sandstone and shale sequences. Outer Makran, located north of Chah Khan thrust (Fig. 2), is made up of Miocene sandstones and marls. Coastal Makran hosts mud volcanoes and represents a wedge-top basin with Late Miocene to Pleistocene shallowing sequences from slope marl to coastal and continental deposits (Fig. 2) (Dolati, 2010). Since the middle Pleistocene, Coastal Makran was affected by vertical movement and normal faulting (Harms et al., 1984). Normal faults, which are not observed in other units, cross-cut lithologies younger than the Late Miocene (Dolati, 2010). Faulted Pliocene-Pleistocene to Holocene marine terraces raised up to 200 m a.s.l., indicating Quaternary uplift of the coast. Uplift rates are increasing from western (0–0.2 mm/a) to eastern Makran (0.5–2 mm/a) (e.g. Page et al., 1979; Reyss et al., 1999).

Pirlgel mud volcano is located ~300 km from the coast of Makran, between Taftan and Bazman volcanoes, west of Sistan suture zone (Tirrul et al., 1983) that is known as Eastern Iranian Ranges (Stöcklin, 1968). In this zone, a Cretaceous–Tertiary orogenic belt separates the Lut continental block of central Iran from the Afghan block to the east (Fig. 3). It was formed by the closure of a relatively short-lived (Campanian to Paleocene), northward-projecting arm of the Neo-Tethys ocean along an easterly dipping subduction zone (Tirrul et al., 1983). Pirlgel is exposed on the core of a faulted anticline delimited by two NW-SE elongated synclines (Fig. 3). The host rocks mainly consist of sandstones with few conglomerates, shales, siltstones and Eocene to Plio-Quaternary dark-gray limestone.

3. Sampling sites

3.1. Borborok

The Borborok mud volcano is located 70 km NW of Chababar. The mud volcano summit consists of one active cone and several deeply eroded non-active cones developed on its outskirts (Fig. 4A and B). It is the oldest mud volcano in this area and it has been continuously active at least since 1989 (Negareh and Khosravi, 2008). During two sampling surveys (July 2016 and November 2017), two 50 cm high gryphons were discharging a dense mud. The gentle and big bubbles showed a tiny oily film (Fig. 4C and D). A fault, bordering the NW margin of the mud volcano summit, delimited a collapse structure

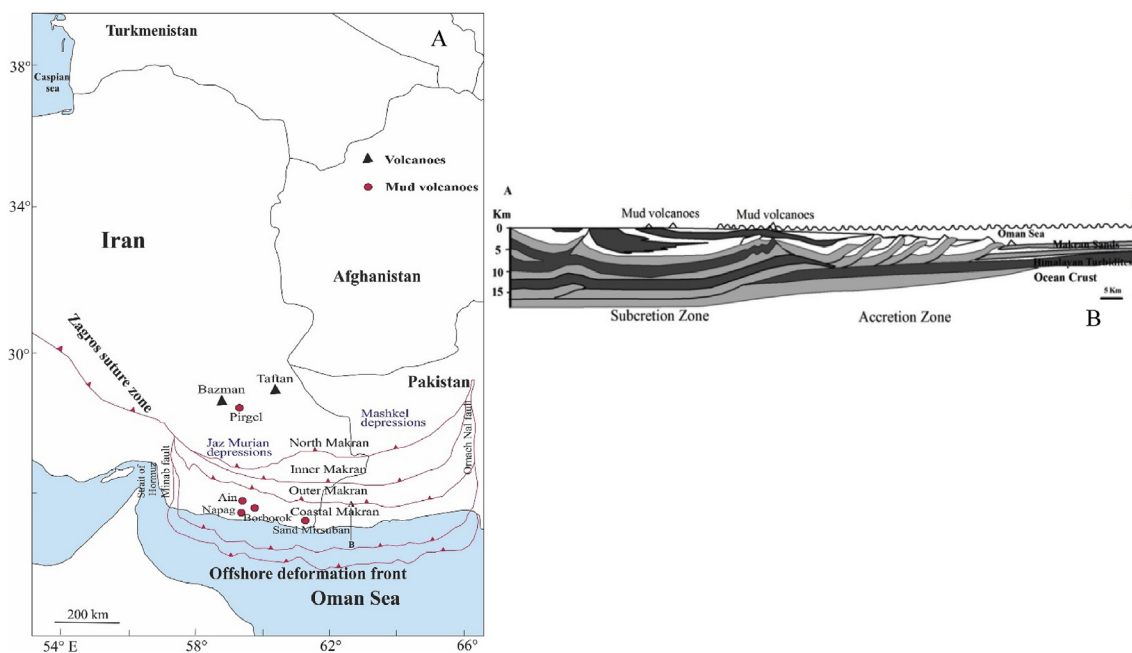


Fig. 1. A) Location of the studied mud volcanoes and Makran structural zone (after Haghypour, 2013), and B) Sketch vertical section along the A-B profile (Hosseini-Barzai and Talbot, 2003).

where active gryphons occurred (Fig. 4E).

3.2. Ain

Ain mud volcano is located 24 km SW of Kahir and 78 km NW of Chabahar, in a flat coastal plain of Oman Sea (Fig. 2). The name Ain means “eye” in Arab and “spring” in Persian and is due to its shape and gurgling. Its morphology is dominated by the presence of an elliptical (52 × 42 m) crater lake (Fig. 5A), unlike most mud volcanoes in the region, which shows a typical a conical shape. Several mud and water pounds were characterized by persistent gas bubbling and located in the outskirts of the mud volcano edifice (Fig. 5B). A strong smell of rotten eggs, indicating the presence of H₂S, was detected during the sampling surveys. The crater lake water was characterized by an intense green color, likely due to the presence of microbial colonies and the occurrence of salt crusts along the rim. Angular clasts and rock fragments (< 10 cm in size) were found in the surroundings, probably being ejected from the lake during eruptive events or detached from the nearby outcrops. On the outskirts of the mud volcano, carbonate deposits, frequently associated with cold CH₄ seeps (Dela Pierre et al., 2010; Diaz-del-Rio et al., 2003; Orpin, 1997), with cylindrical and tubular shapes were observed (Fig. 5C and D). These deposits, likely produced by C-rich fluids discharged from fossil vents controlled by the local faults, cross-cut beds of Quaternary age (Fig. 5C and D), suggesting that the conduits of the uprising fluids were controlled by faults. Owing to the authigenic carbonate deposits generally form in off-shore settings, thus the observed carbonate features around Ain mud volcano likely produced when the area was submerged by the Oman Sea, lately emerged from water by the strong uplift affecting Coastal Makran Zone, indicated by geological evidences (Dolati, 2010; Haghypour, 2013).

3.3. Sand Mirsuban

Sand Mirsuban mud volcano is located 2 km east of Sand Mirsuban and 65 km NW of Chabahar in the coastal plain of Sistan and Balochistan province (Fig. 2). It consists of a 15 m high and 100 m wide asymmetric cone (Fig. 6A). In the summit, a 3 m wide pool (max depth: 6.5 m) was discharging a diluted mud, with an oily film on the surface of the forming bubbles (Fig. 6B). H₂S smelling was also recorded.

3.4. Napag

Napag mud volcano is the biggest structure in the Coastal Makran, with a 35 m high steep-sided main cone whose crater rim has a diameter of 28 m (Fig. 7A and B). It is located 75 km NW of Chabahar and 17 km SW of Kahir (Fig. 2). When compared to the other nearby mud volcanoes, Napag was releasing a much denser mud, as testified by the steep flanks of the main cone. Extruded mudflows were covering an area of 1200 m² around the main structure. The dried mud-streams have a badland appearance (Fig. 7C). Several dried gryphons, representing conduits that were active during past eruptions, were found in the outskirts (Fig. 7D). Small sized (5–10 cm) rock fragments on dried mudflows, likely pertaining to subsurface sequences underneath of the mud volcano (Fig. 7E), were also found. Napag rests in a dormant stage during most of the time (year). The occurrence of high (up to 50 m, according to local witnesses) gas columns and mud eruptions following small and large earthquakes that happened relatively close to Napag suggests a possible relation between mud volcanism and seismicity. Enhanced gas and mud extrusion were also report to occur during tidal and sea turbulences.

3.5. Pirgel

Pirgel mud volcano (Fig. 2), located SE of Bazman volcano and SW of Khash, is the biggest mud volcano in Iran (1400 m wide) (Negarehsh and Khosravi, 2008). During the fieldtrips carried out in July 2016 and November 2017, gas, dense mud and dark oil appearance slicks were emitted by gryphons, pools and cones (Fig. 8A and B). Dormant and active fluid seepages were observed to be oriented along a NW-SE alignment, likely controlled by either an anticline axis or a local/regional fault, as it is shown in Fig. 2. Numerous eroded and dormant gryphons on this volcano testified a past intense activity.

4. Material and methods

Bubbling gas samples from Borborok (3 samples), Ain (5 samples), Sand Mirsuban (5 samples) and Napag (2 samples) were collected using a plastic funnel positioned above the gas emergences connected through a silicon tube to pre-evacuated 300 mL glass flasks equipped

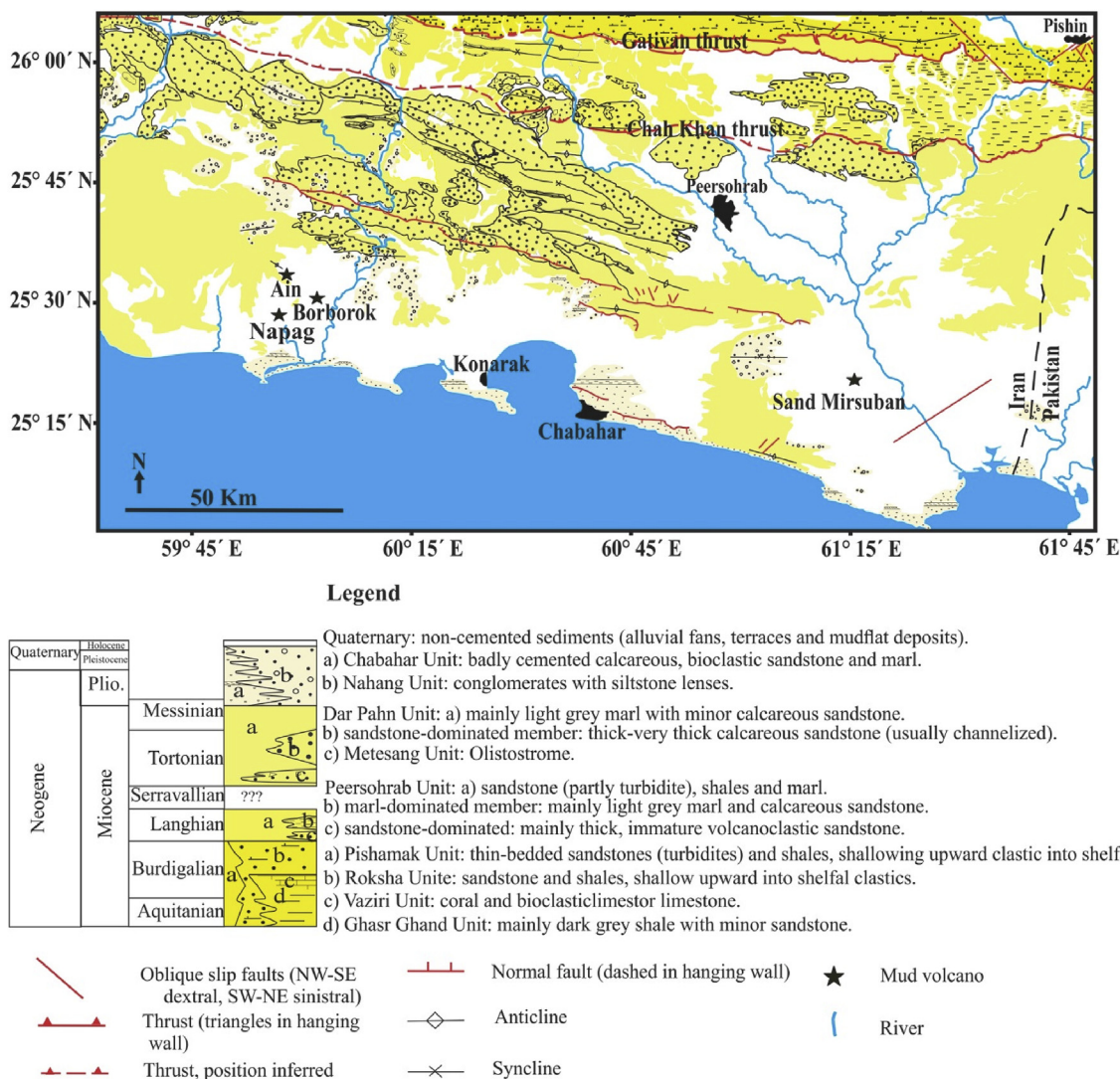


Fig. 2. Location of onshore mud volcanoes on the geological map of Coastal Makran (Modified from Dolati, 2010).

with a thorion valve (Vaselli et al., 2006). The same sampling line was used to collect samples from Pirlgel, although in this case the 300 mL sampling flasks were partly filled with a 4M NaOH solution used to dissolve CO₂ and H₂S and store the low-soluble gases (e.g. hydrocarbons, N₂, O₂ and noble gases) into the flask headspace (Vaselli et al., 2006). Gas samples were analyzed at the Laboratory of Fluid Geochemistry of the Department of Earth Sciences (University of Florence, Italy). C₁–C₄ hydrocarbons and inorganic gases (H₂, Ar, O₂, CO₂ and N₂) were analyzed by using Shimadzu 14A and 15A gas chromatographs, respectively. The former was equipped with a 10 m-long stainless-steel column packed with Chromosorb PAW 80/100 mesh coated with 23% SP 1700 and a Flame Ionization Detector (FID); the latter was equipped with 9 m long molecular sieve column and Thermal Conductivity Detector (TCD).

Carbon dioxide in the gases from Pirlgel was analyzed as CO₃²⁻ in the alkaline solution of the sampling flasks by acidimetric titration (AC) using 0.1 N HCl. The analytical uncertainties were < 10% and < 5% for GC and AC, respectively.

The carbon isotopic ratios (expressed as δ¹³C–CO₂‰ vs. V-PDB) were measured with a Finnigan Delta Plus mass spectrometer after extracting and purifying CO₂ by using liquid N₂ and N₂-trichloroethylene cryogenic traps (Evans et al., 1998; Vaselli et al., 2006). Carrara and San Vincenzo marbles (Internal), as well as NBS18 and NBS19 (International) standards were used to estimate the external

precision. Analytical uncertainty and reproducibility were ± 0.05‰ and ± 0.1‰, respectively. The carbon isotopes in CH₄ (expressed as δ¹³C–CH₄‰ vs. V-PDB) were measured by Cavity Ring-Down Spectroscopy (CRDS) using a Picarro G2201-i Analyzer. The errors of the CRDS analysis was < 1‰. In order to avoid interferences, the instrument inlet line was equipped with (i) a Drierite trap and (ii) a copper trap to remove water vapor and H₂S, respectively. According to the operative ranges of the Picarro G2201-i instrument (up to 500 ppm), gas samples were diluted using a N₂-O₂-Ar gas mixture.

The Helium isotopic ratios (expressed as R/Ra, where R is the ³He/⁴He measured ratio and Ra is the ³He/⁴He ratio in the air: 1.39 × 10⁻⁶; Mamyrin and Tolstikhin, 1984) and those of ⁴He/²⁰Ne were determined by using a double collector mass spectrometer (VG 5400-TFT) according to the method described by Inguaggiato and Rizzo (2004). The analytical error was ± 1%. The R/Ra values were corrected (R_c) for atmospheric contamination using the ⁴He/²⁰Ne ratio (Poreda and Craig, 1989), as follows:

$$R_c/R_a = [(R/R_{a,measured}) - r]/(1 - r) \tag{1}$$

where r is the (⁴He/²⁰Ne)_{air}/⁴He/²⁰Ne_{measured} ratio while that of (⁴He/²⁰Ne)_{air} is 0.421 at the estimated altitude of recharge of approximately 4000 m (Hoke et al., 1994).

Water temperature and pH and were measured *in situ* using an EXTECH® (ExStik® EC500) portable instrument. Precision of the

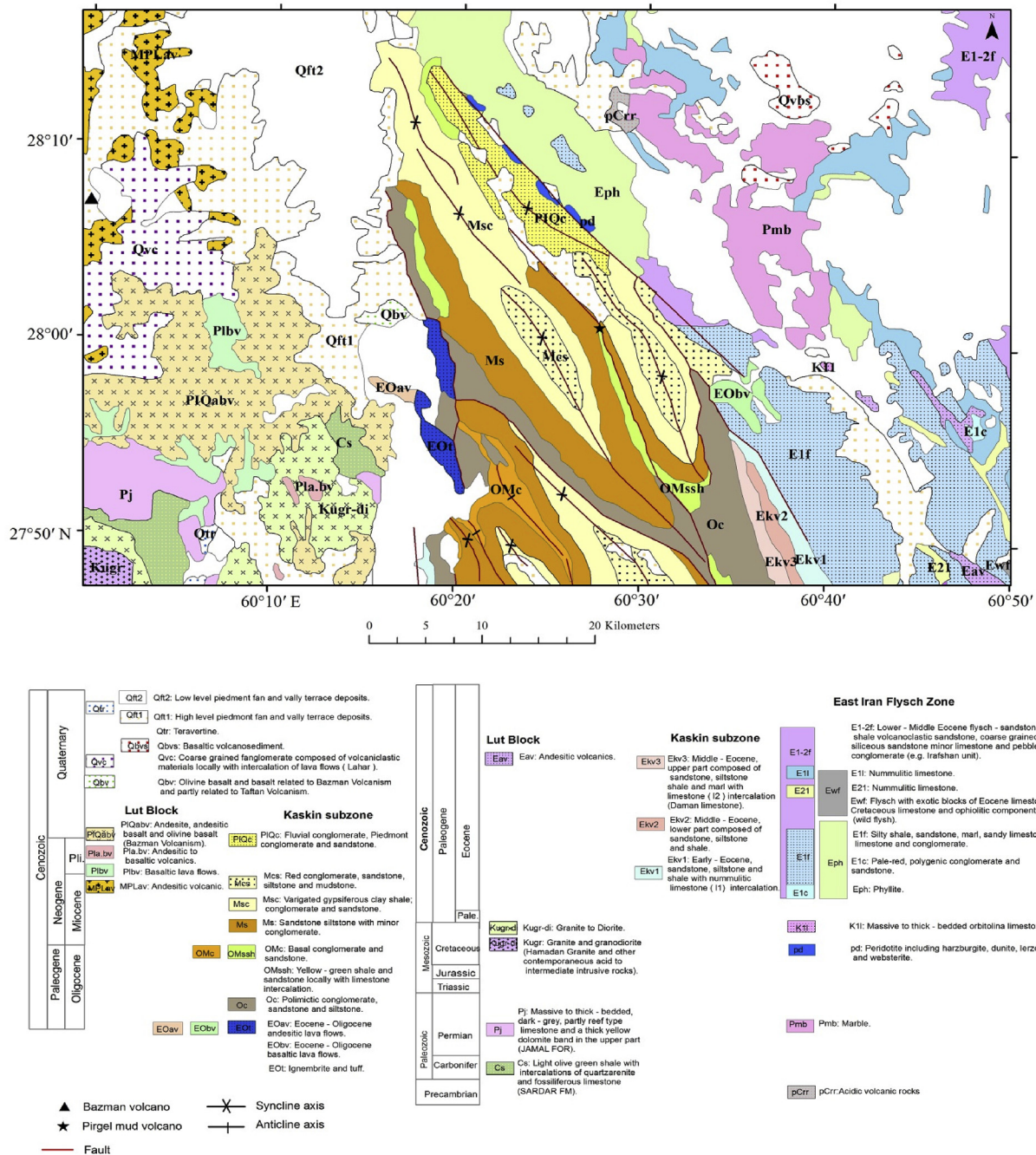


Fig. 3. Geological map of Pirgel mud volcano and surroundings (modified after Aghanabati, 1994 and Sahandi, 1996).

instrument was ± 0.1 and ± 0.5 °C for pH and temperature, respectively. Water was separated from mud by gravity (You et al., 1996), with exception of the Napag samples that were centrifuged due to the presence of dense mud. For each sampling site, 4 aliquots (2 filtered samples – 50 mL each – at 0.45 µm and acidified with 0.5 mL of ultra-pure HCl and HNO₃ for the analysis of major cations and trace elements, respectively; 1 filtered sample – 125 mL – for the analysis of anions and 1 unfiltered sample – 50 mL – for the analysis of water isotopes) were collected in HDPE bottles. Water chemistry was performed at the Iran Mineral Processing Research Center (IMPRC) and Department of Earth Sciences (University of Florence, Italy). Major anions (Cl, SO₄, HCO₃, NO₃, Br and F) and cations (Na, K, Ca, Mg and NH₄) were analyzed using Metrohm 861 and 761 ion chromatography, respectively. Boron was analyzed by molecular spectrophotometry (MS; Beckman DU 520) using the Azomethine-H (AH) method (Bencini,

1985). Analytical errors for IC and MS were ≤ 5%. Trace elements (As, Ba, Co, Cd, Cu, Mn, Fe, Li, Sr, Ni, Si, Zn, Pb and Sb) were analyzed by using an Optima 8000 PerkinElmer Inductively Coupled Plasma Optical Emission Spectrometer (ICP-OES). Analytical error for ICP-OES was ≤ 10%. The ¹⁸O/¹⁶O and ²H/¹H ratios in water (δ¹⁸O–H₂O and δ²H–H₂O ‰ vs. V-SMOW, respectively) were analyzed using a Finnigan MAT Delta plus XP + Gasbench at G.G. Hatch Stable Isotope Laboratory (Faculty of Science, Ottawa University, Canada). Precision (2 sigma) of the isotope analysis was ± 0.15‰ and ± 2.0‰ for δ¹⁸O–H₂O and δD–H₂O, respectively.

X-ray Powder Diffraction (XRD) analyses were carried out at the Department of Earth Sciences of Florence (Italy) using a XRD Philips PW 1050/37 diffractometer with a Philips X'Pert PRO data acquisition and interpretation system, operating at 40 kV-20 mA, with a Cu anode, a graphite monochromator and 2°/min goniometer speed in a 5°-70°θ

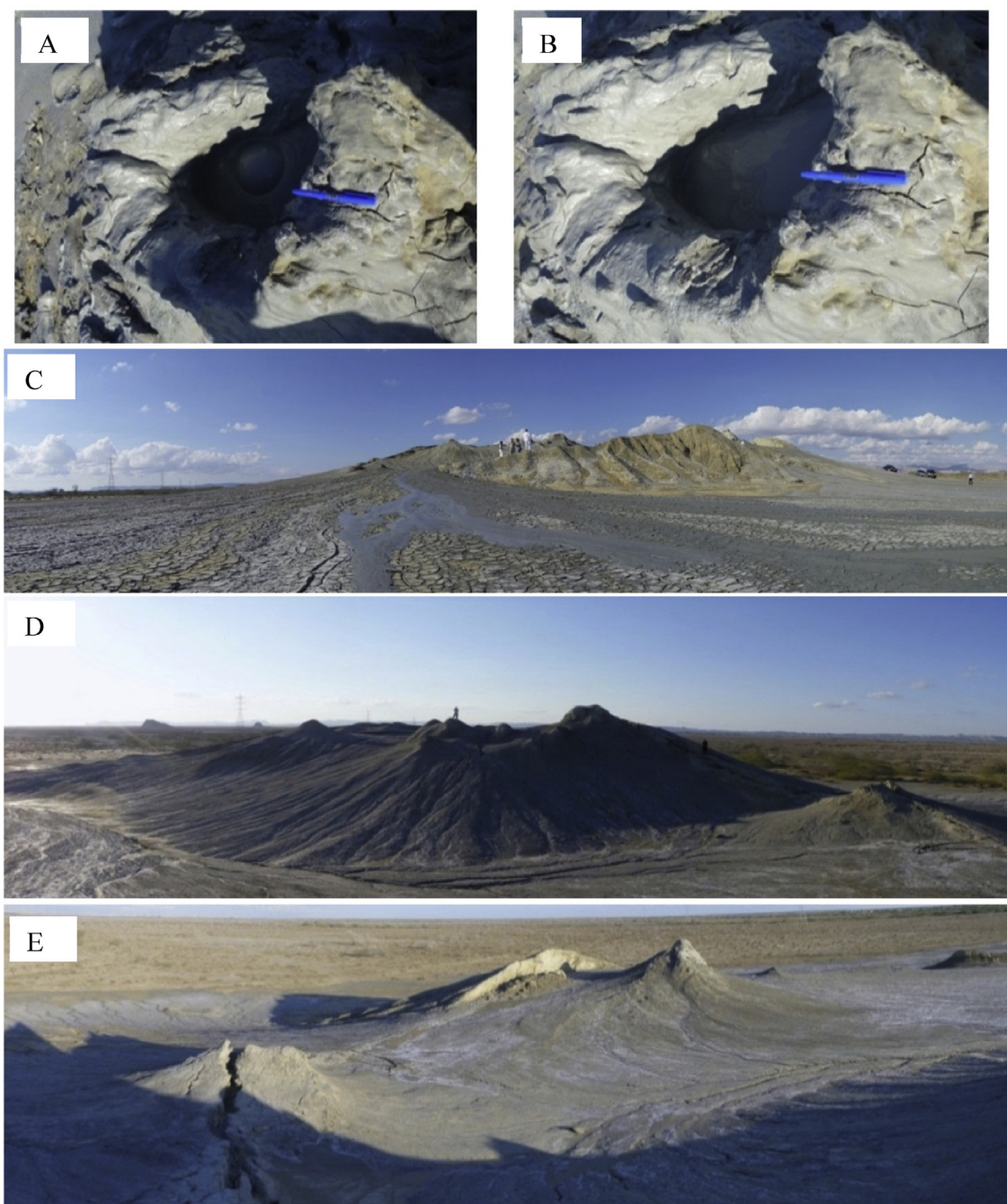


Fig. 4. The active gryphon in the Borborok mud volcano (A and B), the main (C) and the eccentric cones (D). A view of the fault in the NW margin that cross-cuts the mud volcano summit (E).

scanning range for the bulk sample and 5° – 32° for clay fraction. The $< 4 \mu\text{m}$ fraction was separated by transferring about 2 g of powdered mud in a centrifugation tube with 100 mL of MilliQ water. Then, the suspension was placed in an ultrasound bath to disperse the particles. Subsequently, the suspension was centrifuged four times, each time the supernatant was removed, the mud was swirled and 100 mL of MilliQ water was added. Once the last centrifugation was completed and the supernatant discarded, the wet sediments were transferred in a sedimentation graduated cylinders by adding 100 mL MilliQ water. Clay-size fractions separated by gravity separation according to the Stoke's Law and deposited on glass slides. Clay minerals were identified by XRD on air-dried samples by analyzing the following aliquotes: i) untreated, ii) glycolated and iii) heated at 450°C and iv) heated at 650°C in a ventilated stove (Cipriani, 1958a,b; Cipriani and Malesani,

1972).

5. Results

Chemical (in % by vol.) and isotopic composition of CH_4 and CO_2 in the bubbling gases are reported in Table 1. Gases emitted from the on-shore mud volcanoes were dominated by CH_4 , whose concentrations were in a relatively narrow range: from 96.1 to 97.2% at Borborok, from 95.7 to 97.8% at Ain, from 94.3 to 97.8% at Sand Mirsuban and from 96.6 to 97.2% at Napag. Ethane (C_2H_6) was the most abundant C_{2+} compound (up to 3.66%), followed by propane (C_3H_8 ; up to 0.69%) and the C_4 alkane isomers ($i\text{C}_4\text{H}_{10}$ and $n\text{C}_4\text{H}_{10}$; up to 0.45% and 0.25%, respectively). Inorganic gases were $< 5.5\%$ and mainly consisted of N_2 (up to 4.15%) and CO_2 (up to 2.33%), with minor

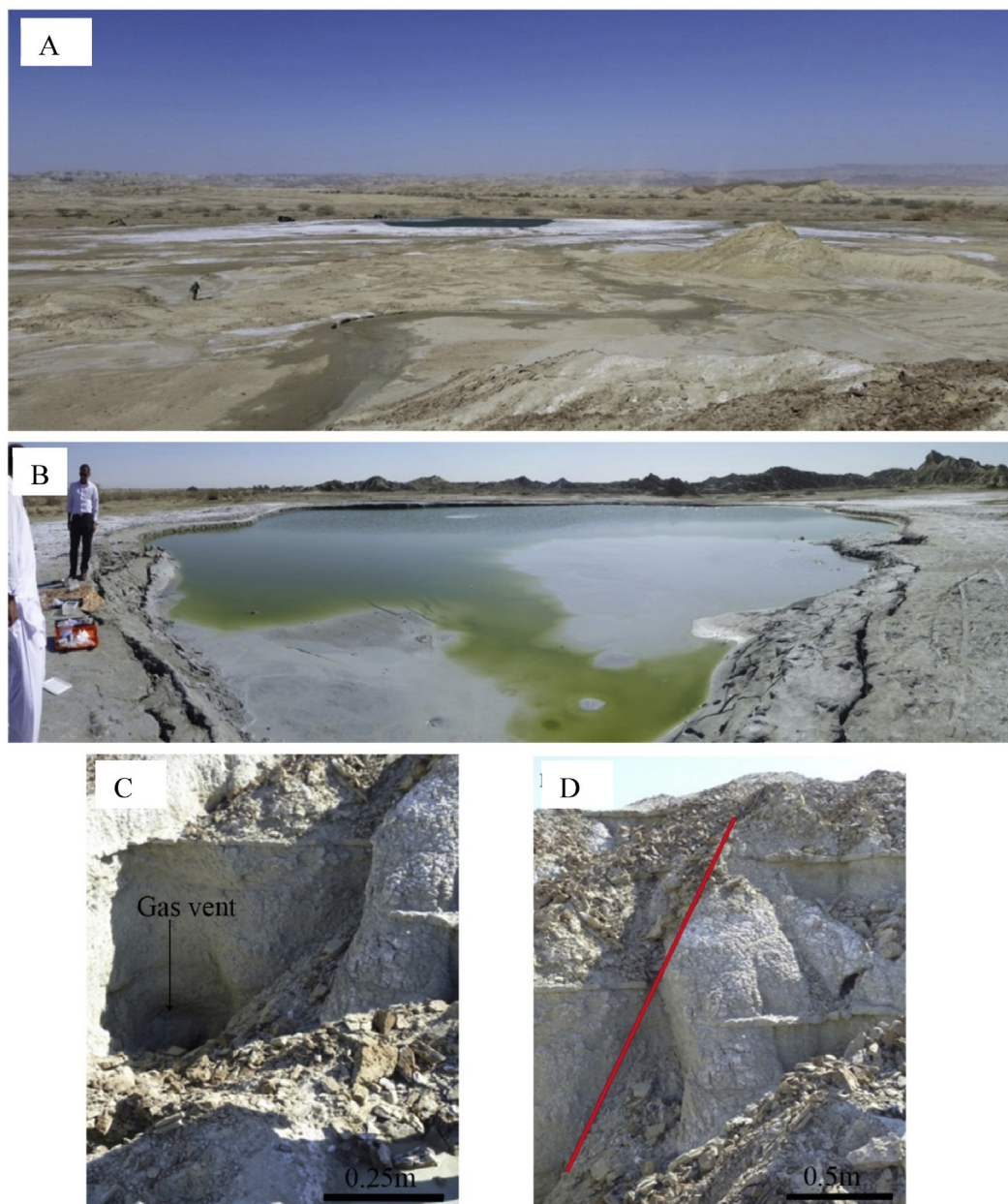


Fig. 5. A) Lateral view of the Ain crater lake, B) bubbling gases within the crater lake, C) gas vent, and D) a fault (red line) that likely acted as a path for the uprising gases. The cylindrical carbonate deposits were possibly formed to the interaction between CH_4 -rich gases and seawater in the past. (For interpretation of the references to color in this figure legend, the reader is referred to the Web version of this article.)

concentrations of O_2 (up to 0.14%), Ar (up to 0.068%) and H_2 (up to 0.026%). The $\delta^{13}\text{C}$ values in CH_4 ranged from -36.1 to -30.2‰ vs. V-PDB, whereas those of CO_2 were in a range from -34.2 to -11.1‰ vs. V-PDB (Table 1).

Gases discharged from Pirgel mud volcano were rich in CO_2 (from 83.9 to 88.7%), with relatively high content of CH_4 (from 9.31 to 12.9%), N_2 (up to 2.08%), C_2H_6 (up to 0.54%), O_2 (up to 0.18%), and minor concentrations ($< 0.1\%$) of Ar, H_2 and $\text{C}_3\text{-C}_4$ alkanes. The $\delta^{13}\text{C}\text{-CH}_4$ and $\delta^{13}\text{C}\text{-CO}_2$ values ranged from -40.7 to -42.2‰ vs. V-PDB and from -11.9 to -13.8‰ vs. V-PDB, respectively, whereas the R/Ra values of the gas samples from Pirgel gryphon and cone were similar, i.e. 1.61 and 1.59, respectively.

The chemical and isotopic composition of the waters is listed in Table 2. Waters from the on-shore mud volcanoes showed a Na-Cl composition, whereas those from Pirgel were Na- HCO_3 . The pH values were ranging from 6.9 to 9.1 (Pirgel), 7.5 to 8.4 (Sand Mirsuban), 8.1 to

8.8 (Ain), 7.9 to 8.3 (Napag) and 8.2 to 8.3 (Borborok). Ain waters showed relatively high concentrations of Cl (up to 52.5 g/L), Br (up to 210 mg/L) and Na (up to 41.8 g/L), whereas lower contents were measured in the other sites (Cl: from 4.8 to 13.9 g/L; Br: from 11 to 40 mg/L; Na: from 4.1 to 10.0 g/L). Pirgel, Ain and Napag waters displayed remarkably high HCO_3 concentration (up to 12,300, 10,200 and 4200 mg/L, respectively). SO_4 concentrations were up to 1800 mg/L, with the exception of one water-dominated from Ain water (4400 mg/L). Ca, Mg and K concentrations were from 11 to 98 mg/L, from 7 to 230 mg/L, and from 48 to 380 mg/L, respectively. Significant concentrations of Li were measured at Pirgel (from 21 to 33 mg/L), Sand Mirsuban and Ain (from 9 to 13 mg/L), whereas in the other sites Li was < 5 mg/L. The concentrations of NH_4 and B ranged from 20 to 380 mg/L and from 160 to 340 mg/L, respectively. Remarkably, at Pirgel Ba and Fe concentrations were up to 12 and 1.3 mg/L, respectively. Waters from Pirgel were also significantly enriched in As (up to



Fig. 6. A) Lateral view of Sand Mirsuban mud volcano asymmetric cone, and B) a mud pond showing oil-related iridescence.

3.4 mg/L). Sr concentrations were up to 21 mg/L, whereas those of Ni, Cu and Zn were relatively low (up to 0.0042, 0.019 and 0.041 mg/L, respectively). Sb (up to 0.11 mg/L), Cd (up to 0.31 mg/L) Co (up to 0.013 mg/L) and Pb (up to 0.032 mg/L) showed the highest contents in one of the water-dominated samples from Ain (Table 2). No significant differences were recorded when the chemical data from two sampling surveys are compared. An increase in the outlet temperature of Napag (41.1 °C) was measured in July 2016, four months after its latest eruption. The $\delta^{18}\text{O}$ values were varying from 7.2 to 13.0‰ vs. V-SMOW whilst those of δD were comprised between -23.8 and 34.2‰ vs. V-SMOW.

Quartz, muscovite, illite, albite, calcite and chlorite were identified in the bulk-muds from all mud volcanoes (Fig. 9). Halite was only found at Pirgel, Borborok and Ain, whereas dolomite was detected at Sand Mirsuban, Napag, Ain and Pirgel. Traces of marcasite were detected in the Sand Mirsuban, Napag and Ain mud samples (Fig. 9). The clay-sized fraction was relatively homogeneous and mainly consisting of illite, chlorite and kaolinite (Fig. 10).

6. Discussion

6.1. Gas origin

The chemical composition of gas samples from mud volcanoes on the Coastal Makran (Table 1) was dominated by CH_4 , the most common gas discharged from mud volcanoes, whereas the Pirgel gas was CO_2 -rich.

Methane from natural gas reservoirs in sedimentary environments may form through either i) processes involving both inorganic and organic compounds related to metabolic and biosynthetic activity of microbes, such as acetate fermentation and CO_2 reduction, occurring at relatively low temperature (< 120 °C, Quigley and MacKenzie, 1988; Takai et al., 2008), or ii) thermogenic decomposition of organic matter buried in sediments (Oremland et al., 1987; Rice and Claypool, 1981; Schoell, 1980, 1988; Whiticar et al., 1986; Whiticar, 1999). These two production mechanisms can be distinguished according to the isotopic composition of methane (Schoell, 1980) and by combining these isotopic parameters with the C_1/C_{2+} ratio (Bernard et al., 1978; Whiticar, 1999). Strongly negative $\delta^{13}\text{C}\text{-CH}_4$ and $\delta\text{D}\text{-CH}_4$ values (< -50 ‰ V-PDB and < -150 ‰ V-SMOW, respectively) and C_1/C_{2+} ratios > 1000 are commonly interpreted as produced by biogenic processes, whereas heavier isotopes and C_1/C_{2+} ratios < 100 can be regarded as related to a thermogenic origin. Accordingly, the $\delta^{13}\text{C}\text{-CH}_4$ values (from -42.2 to -30.2 ‰ V-PDB) and relatively low C_1/C_{2+} ratios (< 100) shown by the gas samples of the present study are indicative of a prevailing CH_4 production through thermogenic degradation of organic matter with no

significant contribution of biogenic methane (Fig. 11; Bernard et al., 1978). Noteworthy, CH_4 in fluids from two on-shore mud volcanoes in Makran of Pakistan, here reported for comparison, displayed a biogenic source (Delisle et al., 2002) (Fig. 11). This is quite surprising, since the Iran and Pakistan mud volcanoes are related to the same tectonic zone. Nevertheless, the widespread presence of gas seepage containing traces of C_{2+} hydrocarbons, oil seepage in the Makran coast of Pakistan and abundant bright spots on off-shore seismic lines were reported (Harms et al., 1982; White, 1979). These features suggest that hydrocarbons generated from thermally-mature source rocks. The difference in gas source may be caused by molecular fractionation (Mazzini and Etiope, 2017), a process invoked to explain the relatively high C_1/C_{2+} ratios of gases emitted by mud volcanoes of Pakistan (Delisle et al., 2002) which mimic the features of a biogenic source.

It is worth noting that liquid petroleum is produced during progressive thermal degradation of kerogen in catagenesis stage where thermogenic CH_4 also occurs (Hunt, 1996; Tissot and Welte, 1978). Therefore, the oily films observed at Borborok, Sand Mirsuban and Pirgel can be interpreted as a further evidence for a thermogenic origin of the hydrocarbons from SE Iran mud volcanoes.

The few available data of total organic carbon (TOC) from stratigraphic horizons in the Pakistan sector of the Makran accretionary prisms (Khan et al., 1991) suggest that potential source rocks (Types II and III) in this area are, as follows: 1) shales in the Talar Formation of Mio-Pliocene age, 2) shales in the Hoshab trench deposits of Middle Eocene to Early Oligocene age and 3) the Parkini mudstones of Middle to Late Miocene age. The latter act as mud source for the active on-shore mud volcanoes of Pakistan Makran (Delisle et al., 2002). No geochemical data on the Eocene-Miocene rocks from both Iranian Makran accretionary prisms and Kaskin subzone (Figs. 2 and 3) are available, although these formations may be representing a hydrocarbon source.

Carbon dioxide in CH_4 -rich gas reservoirs is produced by a variety of biotic and abiotic processes such as oxidation of organic matter, microbial and thermogenic alteration of organic matter, hydrocarbon oxidation by mineralized waters, decarbonation of carbonates, carbonate hydrolysis and endogenic activities (Wycherley et al., 1999). Different CO_2 sources can be recognized based on the $^{13}\text{C}/^{12}\text{C}$ ratios: 0‰ vs. V-PDB, < -20 ‰ vs. V-PDB and -6.5 ± 2.5 ‰ vs. V-PDB for marine limestone, alteration of organic material and Mid-Oceanic Ridge Basalts (MORB), respectively (Sano and Marty, 1995). At a first approximation, the measured $\delta^{13}\text{C}\text{-CO}_2$ values (from -11.9 to -13.8 ‰ vs. V-PDB) measured in the CO_2 -rich Pirgel gases are intermediate between those typical of mantle and a biogenic source. The R/Ra values of these gases were ~ 1.6 R/Ra, with low air contamination as indicated by the high He/Ne ratios (14–257, Table 1). Considering the R/Ra value



Fig. 7. A) Lateral view of Napag mud volcano; B) crater summit of main cone with extruded dense mud. Gas bubbling is randomly scattered along the mud volcano flanks, C) dried mudflow around the main cone, D) dried gryphons, and E) the ejected rock fragments during the previous eruptions within the dried mudflows.

of gases from subduction-related volcanisms (6.5 R/Ra; Hilton et al., 2002) as the deep endmember and the R/Ra value for crustal gases (0.01; Ballentine and Burnard, 2002), the fraction of mantle He is estimated at $\sim 25\%$. The $\text{CO}_2/{}^3\text{He}$ ratios, ranging from 20×10^9 to 30×10^9 , i.e. slightly higher than that typically measured for MORB (2×10^9 – 1×10^{10} , e.g. Marty et al., 1989; Sano and Marty, 1995; Sano and Williams, 1996), coupled with the above mentioned the $\delta^{13}\text{C}$ - CO_2 values, suggest that the origin of the CO_2 discharged from this mud volcano is related to both biogenic and volcanic sources.

6.2. Process governing the chemistry of waters

To provide information on the origin of waters, the $\delta^{18}\text{O}$ - H_2O and δD - H_2O values were compared with those of the Local Meteoric Water Line (LMWL) (Shamsi and Kazemi, 2014) and seawater (Fig. 12). The isotopic composition of waters from (i) two cold springs of meteoric

origin, (ii) two thermal springs showing contribution of geothermal fluids in the southeastern flank of Taftan (Shakeri et al., 2008) and (iii) one thermal spring in the southern flank of Bazman (unpublished data) were also reported for comparison. All the investigated waters were marked by a significant positive $\delta^{18}\text{O}$ -shift with respect to seawater. The two highly saline Ain waters were also characterized by a significant positive shift of the δD - H_2O values. Waters from mud volcanoes commonly show an ^{18}O enrichment caused by rock-water isotopic exchange (Dählmann and de Lange, 2003; Hensen et al., 2015; Scholz et al., 2010). Illitization, typically affecting clay minerals at temperatures ranging from 60°C to 160°C , can cause an increase in terms of $\delta^{18}\text{O}$ - H_2O and a decrease for δD - H_2O (Dählmann and de Lange, 2003). Thus, the waters from the study areas possibly originated from seawater trapped in sediments and affected by isotope fractionation due to water-rock interaction processes. However, contribution of meteoric water affected by $\delta^{18}\text{O}$ and δD fractionation cannot be excluded. A fingerprint



Fig. 8. A) Lateral view of Pirgel mud volcano and NW-SW-aligned active fluid seeping structures, B) gas bubbling pool discharging gray mud and dark oily slicks, and C) a dried gryphon.

Table 1

Chemical and isotopic composition of gases discharged from the Borborok, Ain, Sand Mirsuban and Napag mud volcanoes in the Costal Makran and Pirgel located between two volcanoes. Gas concentrations are given in vol. % and $\delta^{13}\text{C}$ in CO_2 and CH_4 are expressed as ‰ V-PDB.

Locations	Type	Sample no.	CH_4	CO_2	N_2	Ar	O_2	H_2	C_2H_6	C_3H_8	iC_4H_{10}	nC_4H_{10}	$\delta^{13}\text{C}\text{-CO}_2$	$\delta^{13}\text{C}\text{-CH}_4$	C_1/C_{2+}	R/Ra	He/Ne
Pirgel	Gryphon	PG1	11.7	85.6	1.96	0.046	0.13	0.0027	0.43	0.063	0.03	0.016	-13.5	-42.2	22	1.61	257
		PG2	9.31	88.7	1.28	0.028	0.088	0.0026	0.44	0.051	0.027	0.019	-11.9	-40.7	17	-	-
	Cone	PG3	12.9	83.9	2.08	0.05	0.18	0.0024	0.54	0.098	0.052	0.024	-13.8	-41.6	18	1.59	14
Borborok	Gryphon	B-1A	96.1	1.15	2.11	0.046	0.61	0.015	1.15	0.23	0.11	0.06	-34.2	-33.3	62	-	-
		B-1B	96.8	1.55	1.55	0.028	0.062	0.023	1.26	0.25	0.12	0.05	-30.4	-33.5	58	-	-
		B-1C	97.2	1.03	1.66	0.025	0.038	0.019	3.66	0.52	0.23	0.15	-25.3	-32.8	21	-	-
Ain	Salsa	A-1A	97.8	0.91	1.22	0.031	0.046	0.015	2.55	0.69	0.45	0.19	-11.3	-35.2	25	-	-
		A-1B	95.8	0.85	3.12	0.052	0.14	0.011	2.78	0.48	0.26	0.21	-14.0	-36.1	26	-	-
		A-1C	97.8	0.78	1.36	0.026	0.051	0.016	1.69	0.29	0.15	0.11	-12.9	-34.9	44	-	-
		A-1D	95.7	2.33	1.91	0.024	0.021	0.012	3.11	0.66	0.36	0.22	-14.3	-35.4	22	-	-
		A-1E	95.7	1.56	2.65	0.039	0.091	0.016	3.26	0.69	0.33	0.25	-	-34.9	21	-	-
Sand Mirsuban	Pool	S-1A	96.2	1.63	2.08	0.032	0.085	0.021	1.87	0.42	0.31	0.18	-	-31.6	35	-	-
		S-1B	94.9	1.36	3.54	0.057	0.13	0.026	1.55	0.38	0.29	0.11	-	-31.4	41	-	-
		S-1C	97.8	0.96	1.15	0.025	0.039	0.014	1.66	0.46	0.23	0.16	-11.1	-30.9	39	-	-
		S-1D	96.7	1.11	2.05	0.035	0.038	0.009	1.32	0.29	0.18	0.15	-13.2	-32.1	50	-	-
		S-1E	94.3	1.36	4.15	0.068	0.11	0.013	1.78	0.33	0.16	0.14	-	-31.5	39	-	-
Napag	Cone	N-1A	96.6	1.11	2.15	0.036	0.093	0.015	2.11	0.39	0.25	0.13	-12.1	-30.2	33	-	-
		N-1B	97.2	1.55	1.14	0.025	0.041	0.018	1.87	0.41	0.19	0.15	-15.2	-30.6	37	-	-

of evaporation process is reflected by the isotope composition of the two Ain D-rich waters, as also suggested by the high Cl and Br contents (Fig. 13).

The Na-Cl composition of the Ain, Sand Mirsuban, Napag and Borborok waters is typically found in mud volcanoes worldwide (e.g. Mazzini et al., 2009; Oppo et al., 2014; Ray et al., 2013). The relatively high HCO_3^- concentration measured in the Na- HCO_3^- waters from Pirgel (Table 2) can likely be due to dissolution of CO_2 (Minissale et al., 2000;

Younger, 2007), that is the dominant gas compound in gases associated with these waters (Table 1), whereas the excess of HCO_3^- with respect to the stoichiometric ratio with Ca + Mg (Fig. 14) shown by the other waters was possibly caused by Na-Ca exchange with rocks.

Chloride can be regarded as a chemically conservative ion (Motyka et al., 1993), thus element/chloride ratio can be a valuable tool to decipher the fluid sources. All waters are characterized by high B/Cl, Li/Cl, and Na/Cl ratios and low Ca/Cl, Mg/Cl and K/Cl ratio when

Table 2
 Temperature, pH and chemical and isotopic composition of waters collected from four onshore mud volcanoes and that of located between Taftan and Bazman volcanoes in different time periods. The major and trace elements in seawater is from Fontes and Matray (1993) and Masson (1966), respectively.

Mud volcanoes	Type	Sampling year	T (°C)	pH	HCO ₃ ⁻ (mg/L)	F (mg/L)	Cl (g/L)	Br (mg/L)	NO ₃ ⁻ (mg/L)	SO ₄ ⁻ (mg/L)	Ca (mg/L)	Mg (mg/L)	Na (g/L)	K (mg/L)	NH ₄ ⁺ (mg/L)	B (mg/L)	Li (mg/L)	Ca/Cl
Pirgel	Pool	2016	24.7	6.9	8800	2	7.7	19	5.9	600	34	140	8.4	240	60	340	25	0.004
		2017	29.3	8.3	12300	56	8.5	20	36	1800	60	230	10.0	250	130	330	33	0.007
Gryphon	Gryphon	2016	24.1	7.3	9900	32	7.5	11	9.6	1000	64	180	9.9	230	170	330	20	0.008
		2017	28.6	9.1	8900	16	6.2	13	3.6	1700	72	150	7.8	200	380	330	21	0.011
Sand Mirsuban	Pool	2016	24.8	7.5	800	2	13.1	39	4.1	500	72	48	9.5	96	70	170	9	0.005
		2017	26.1	8.4	1100	25	13.9	40	9.6	1700	98	54	9.7	98	380	190	11	0.007
Ain (water dominated)	Salsa	2016	26.4	8.8	10200	20	52.5	210	4.8	1600	20	21	41.8	350	40	310	13	0.0003
		2017	25.1	8.1	5800	28	32.6	110	42	4400	37	24	26.6	150	170	320	13	0.001
Ain (mud dominated)	Salsa	2016	26.4	8.8	1200	3	7.8	26	2.6	700	11	7	6.0	48	20	220	2	0.001
		2017	23.5	8.5	1800	25	9.4	35	28	1700	16	10	7.6	52	270	280	3	0.002
Napag	Pool	2016	41.1	8.3	4200	3	6.5	20	1	500	25	22	5.7	54	30	160	4	0.004
		2017	24.3	7.9	3400	3	6.8	21	2.1	-	-	19	5.6	67	30	170	5	0.004
Borborok	Gryphon	2016	29.2	8.3	1200	2	5.8	19	6.6	900	23	27	4.7	40	20	200	2	0.004
		2017	24.2	8.2	1500	14	4.8	19	9.8	1200	26	23	4.1	32	130	190	4	0.005
Seawater	-	-	-	-	140	1.3	19.5	67	0.5	2600	412	1290	10.8	380	0.07	4.6	0.18	0.021

Mg/Cl	Na/Cl	B/Cl	Sr/Cl	HCO ₃ ⁻ /Cl	K/Cl	Li/Cl	K/Cl	HCO ₃ ⁻ /Cl	Sr (mg/L)	Fe (mg/L)	Ni (mg/L)	Cu (mg/L)	Zn (mg/L)	As (mg/L)	Sb (mg/L)	Co (mg/L)	Cd (mg/L)	Si (mg/L)	Pb (mg/L)	δ ¹⁸ O (‰)	δD (‰)
0.018	1.09	0.01	6	1.1	0.003	0.003	0.03	1.1	6	0.09	0.0042	0.002	0.008	1.9	0.03	0.003	0.0050	13	0.009	9.9	-18.1
0.027	1.17	0.005	7	1.4	0.004	0.004	0.03	1.4	7	0.08	0.0040	0.013	0.028	1.2	0.03	0.004	0.0063	13	0.006	9.5	-23.8
0.024	1.32	0.005	5	1.3	0.003	0.003	0.03	1.3	5	1.3	0.0041	0.007	0.012	2.9	0.03	0.007	0.0093	11	0.011	10.3	-17.9
0.024	1.25	0.004	7	1.4	0.0033	0.0033	0.03	1.4	7	0.9	0.0032	0.008	0.028	3.4	0.03	0.006	0.0086	13	0.017	12.1	-15.1
0.004	0.72	0.002	19	0.6	0.0007	0.0007	0.06	0.1	19	0.1	-	0.002	0.004	0.05	0.02	0.003	0.0002	6	0.004	7.8	-9.0
0.004	0.69	0.002	20	0.8	0.0007	0.0007	0.08	0.2	20	0.06	-	0.002	0.004	0.04	0.02	0.002	0.0002	6	0.005	8.1	-10.1
0.0004	0.79	0.015	21	0.2	0.0002	0.0002	0.2	0.9	21	0.9	0.0002	0.019	0.038	0.2	0.09	0.010	0.31	11	0.028	11.8	34.2
0.0007	0.81	0.009	12	0.2	0.0003	0.0003	0.2	1	12	1	0.0003	0.018	0.041	0.1	0.11	0.013	0.25	11	0.032	10.9	33.9
0.0008	0.76	0.02	4	0.1	0.0002	0.0002	0.1	0.01	4	0.01	0.0006	0.002	0.003	0.04	0.02	0.003	-	9	0.002	7.2	-7.4
0.001	0.80	0.017	4	0.1	0.0003	0.0003	0.1	0.07	4	0.07	0.0007	0.009	0.002	0.03	0.01	0.002	-	10	0.001	8.2	-9.3
0.003	0.87	0.006	6	0.6	0.0006	0.0006	0.6	0.06	6	0.06	0.0018	0.013	0.031	0.02	0.01	0.005	-	8	0.003	13.0	-0.8
0.002	0.82	0.006	6	0.5	0.0007	0.0007	0.5	0.4	6	0.4	0.0016	0.012	0.024	0.04	0.01	0.003	-	7	-	12.6	-1.1
0.004	0.81	0.009	5	0.2	0.0003	0.0003	0.2	0.08	5	0.08	0.0014	0.003	0.008	0.04	0.03	0.003	0.002	7	0.002	8.9	-11.0
0.004	0.85	0.007	5	0.3	0.0008	0.0008	0.3	0.4	5	0.4	0.0020	0.009	0.007	0.04	0.04	0.004	0.001	7	0.015	9.8	-13.8
0.066	0.55	1.1E-05	8	0.007	0.019	0.007	0.007	0.01	8	0.01	0.0020	0.003	0.01	0.0004	0.0003	0.0004	0.0001	-	3E-05	-	-

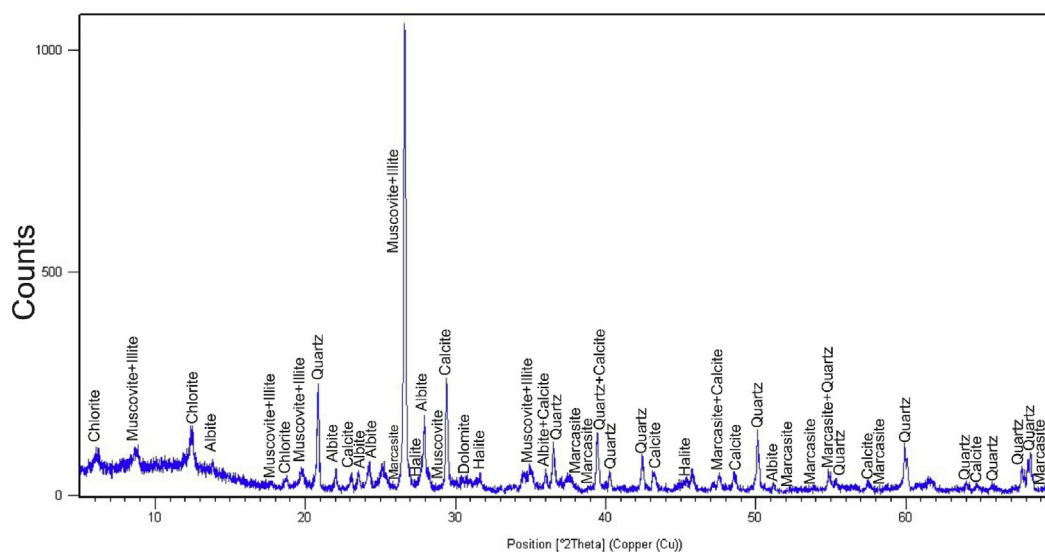


Fig. 9. Representative X-ray diffractograms (Ain mud volcano) for whole mud matrix of mud volcanoes from Iranian Makran.

compared to those in seawater (Fig. 15). These geochemical features were commonly observed in waters from mud volcanoes worldwide and ascribed to water-rock interaction with marine sediments (Aloisi et al., 2004; Chao et al., 2011; Hensen et al., 2004, 2007; Lavrushin et al., 2005; Mazzini et al., 2009; Teichert et al., 2005; Williams et al., 2001; You et al., 2004). High B can be due to smectite to illite conversion at great depth, where this process is favored by temperature (Colten-Bradley, 1987; Kharaka and Hanor, 2004; Kopf and Deyhle, 2002; Williams et al., 2001; You et al., 1996). The lack of smectite shown by X-ray analysis of mud samples seems to confirm this hypothesis although it could also be hypothesized that the mud source was smectite-free. Strong water-rock interactions, implying a long water circulation pattern, is supported by the relatively high Li concentrations (Table 2 and Fig. 15). Hydrothermal fluids are regarded as one of the sources of fluid-mobile elements such as B and Li discharged from volcanic systems to the surrounding environments (Arnórrsson and Andrésdóttir, 1995; James et al., 1999; Scholz et al., 2010; Wrage et al., 2017). It could be suggested that the observed higher contents of B and Li in

waters from Pírgel with respect to those of other mud volcanoes (Table 2) indicating that the fluids from clay dehydration are likely mixed with volcanic hydrothermal solutions.

Arsenic is a ubiquitous component in many geothermal waters and its surface manifestations such as hot springs around the world (Bundschuh and Maity, 2015; López et al., 2012; Webster and Nordstrom, 2003). Pírgel waters were characterized by high As concentrations (up to 3.4 mg/L) (Table 2), which are similar to those determined in waters associated discharged from the nearby Taftan and Bazman volcanoes (up to 3.8 mg/L; Shakeri et al., 2014), suggesting that As is mainly sourced by hydrothermal fluids. This geochemical feature, as also supported by (i) the occurrence of significant mantle He, (ii) the mantle-like $\text{CO}_2/{}^3\text{He}$ ratios and (iii) the CO_2 -dominated composition of gases discharged, suggest to consider Pírgel as an atypical mud volcano, similar to those reported in various sedimentary basins linked with igneous intrusions and high temperature geothermal fluids (Ciotoli et al., 2016; Holford et al., 2013; Mazzini et al., 2011). The occurrence of thermogenic hydrocarbons in the Pírgel gases (Fig. 11)

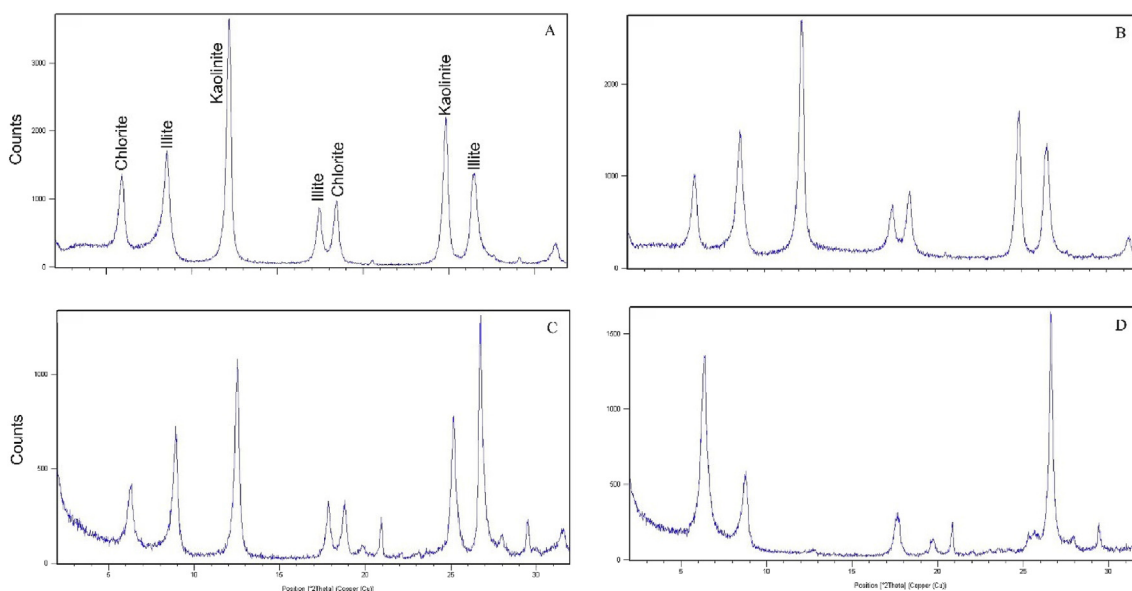


Fig. 10. X-ray diffractograms of a representative mud sample showing diffractograms for untreated (A), glycolated (B) and heated up to 450 °C (C) and up to 650 °C (D) of oriented clay fraction.

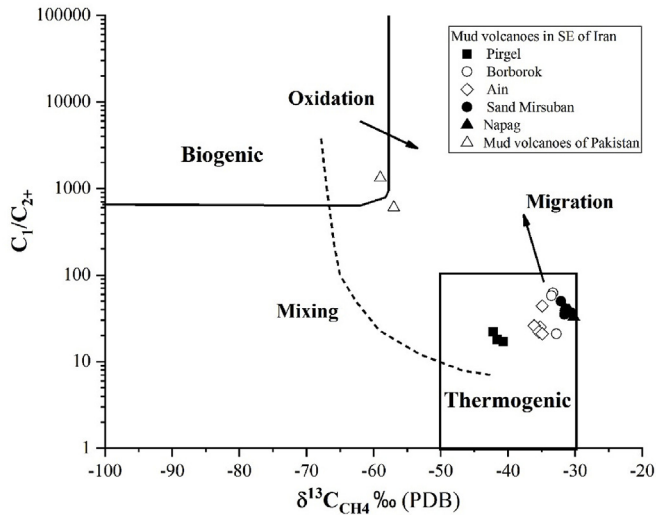


Fig. 11. $C_1/(C_{2+})$ vs. $\delta^{13}C_{CH_4}$ diagram (Bernard et al., 1978) for the gases from the Borborok, Ain, Sand Mirsuban, Napag and Pirgel mud volcanoes. The composition of two on-shore gas samples from Pakistan Makran mud volcanoes is reported for comparison.

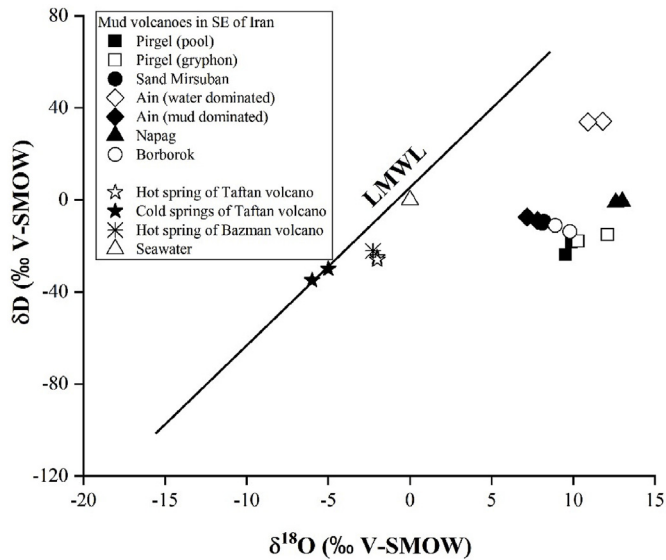


Fig. 12. $\delta D-H_2O$ vs. $\delta^{18}O-H_2O$ diagram of waters from mud volcanoes in SE Iran, hot and cold spring waters around the Taftan volcano (Shakeri et al., 2008) and hot spring waters around the Bazman volcano (unpublished data). The local meteoric water line (LMWL; Shamsi and Kazemi, 2014) is also reported.

suggests that in this area organic-rich sedimentary rocks interact with CO_2 -rich hydrothermal fluids from the adjacent volcanic systems. The relatively high HCO_3 content of Pirgel water, likely deriving from CO_2 dissolution, may also enhance the mobilization of arsenic through the formation of arseno-carbonate complexes (Bhattacharya et al., 2006; Kim et al., 2000, 2003). The organic matter-rich, fine-grained sediments producing hydrocarbon components may act as possible As source (Paikaray, 2012; Simmons et al., 2016) to waters from Pirgel in addition to As input of geothermal fluids.

6.3. Geothermometry

To evaluate the depth of fluid reservoir(s), geothermometers based on the composition of the main cations are usually applied. The reservoir(s) temperature of the water samples of Makran mud volcanoes

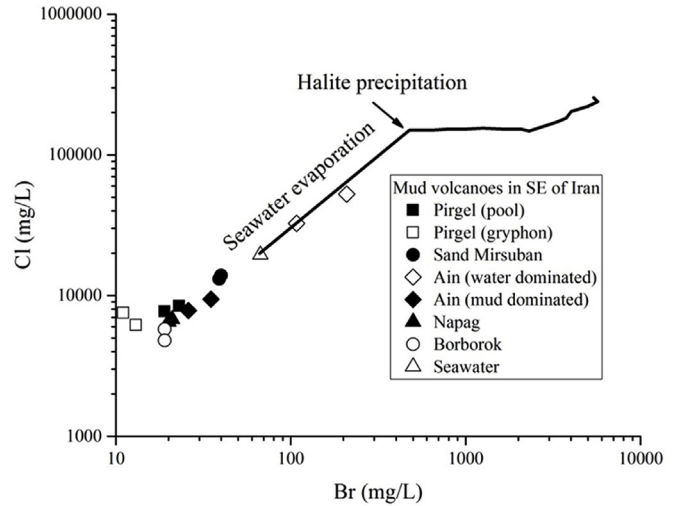


Fig. 13. Cl/Br plot for waters from mud volcanoes in SE of Iran.

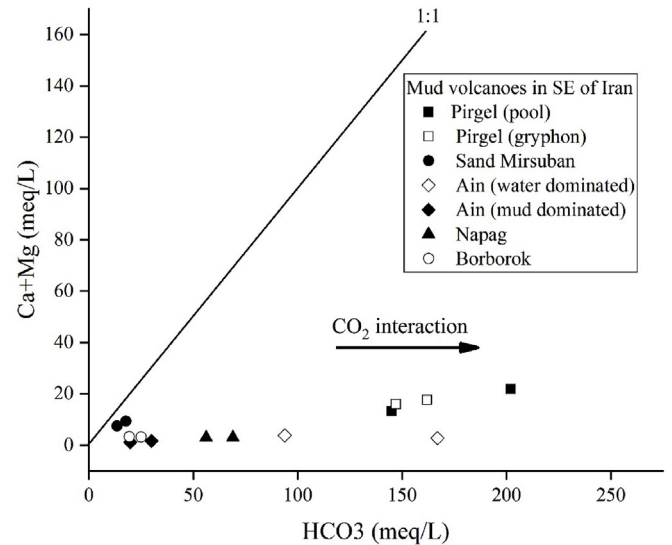


Fig. 14. Ca + Mg vs. HCO_3 binary diagram for waters from mud volcanoes of SE Iran.

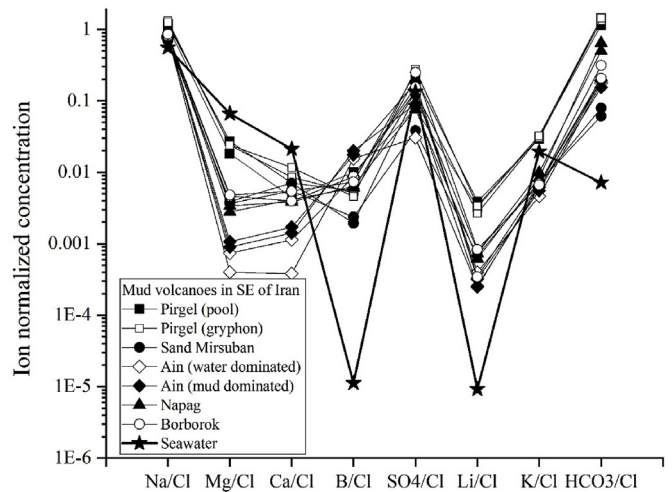


Fig. 15. Ion/Cl ratio of waters expelled from mud volcanoes of SE Iran. Seawater is also showed for comparison.

Table 3
Calculated temperatures (°C) using cation geothermometers.

Mud volcanoes	Type	Na-Li ^a	Na-Li ^b	Na-K	Mg-Li	Mg-K
Pirgel	Pool	–	155	129	154	114
		–	163	121	156	108
	Gryphon	–	127	117	142	109
		–	147	123	147	107
Sand Mirsuban	Pool	218	–	77	138	103
		234	–	77	142	102
Ain (water dominated)	Salsa	141	–	69	165	158
		169	–	53	163	127
Ain (mud dominated)	Salsa	–	35	67	120	111
		–	42	60	127	108
Napag	Pool	–	68	74	124	98
		–	80	84	133	106
Borborok	Gryphon	–	45	69	101	87
		–	84	66	123	84

^a Cl > 0.3 mol/L.

^b Cl < 0.3 mol/L.

calculated by cation geothermometers such as Na-Li (for low and high salinity waters with Cl < 0.3 and Cl > 0.3 mol/L, respectively), Na-K (Verma and Santoyo, 1997), Mg-Li (Kharaka and Mariner, 1989) and Mg-K geothermometers (Giggenbach, 1988) are reported in Table 3. The Na-Li and Na-K geothermometers provide extremely low temperature estimations (Table 3) probably due to the influence of seawater coupled with the low kinetics of the chemical reactions at the basis of these geothermometers that prevents the attainment of a complete equilibrium. Mg-Li and Mg-K geothermometers, which are both characterized by a relatively fast kinetics, seem to indicate reliable temperatures for onshore mud volcanoes, ranging from 101 to 165 °C and 84–158 °C, respectively. These estimated temperatures are consistent with those favoring the smectite-to-illite transformation process (Kastner et al., 1991; Moore and Vrolijk, 1992). Calculated temperature for the Pirgel fluids ranged from 107 °C (Mg-K geothermometer) to 163 °C (Na/Li geothermometer), thus in the same range of those estimated for the other mud volcanoes in this study. On this basis, it seems that the relatively close Taftan and Bazman volcanoes have no influence on the temperature of the Pirgel fluid source. Notwithstanding the uncertainty of such a theoretical approach, the depth of the fluid source of these mud volcanoes can be tentatively computed. Considering an average geothermal gradient of 20 °C/1000 m, as measured in drilled wells in on-shore Pakistani Makran (Harms et al., 1984; Khan et al., 1991), and an average ground temperature of 26 °C, the main fluid source is located at 3–7 km depth for onshore mud volcanoes. Unfortunately, no information on the geothermal gradient close to Taftan and Bazman volcanoes is available, although it is plausible to hypothesize the occurrence of a thermal anomaly with respect to Coastal Makran. Considering this assumption, root of this mud volcano should be shallower than those calculated for onshore mud volcanoes.

It is worth noting that the obtained depth estimations are in agreement with a seismic survey on offshore accretionary complex of Iranian Makran revealing that root of shale diapirs and mud volcanoes is more than 3 km (Grando and McClay, 2007). Whereas, the fluid reservoir of mud volcanoes within the Makran accretionary prisms of Pakistan, emitting biogenic gases, was estimated at 2–3 km depth (Delisle et al., 2002).

6.3.1. Concluding remarks

Chemical and isotopic composition of light alkanes consistently indicated that the hydrocarbons discharged from four investigated mud volcanoes in the Iranian Makran accretionary prisms and Pirgel (situated between the igneous volcanoes of Taftan and Bazman) have a thermogenic source. The hydrocarbon genetic process is likely related to chemical-physical conditions occurring in the Coastal Makran at depth, e.g. high pressure and relatively low temperature, dictated by

subduction-related process at the accretionary wedge origin. Differently, the CO₂-rich gases characterizing Pirgel volcano probably originated from both thermal degradation of sedimentary organics and hydrothermal fluids from the neighboring volcanic complex.

Two main water types in the studied volcanic systems from SE Iran, i.e. i) Na-Cl, expelled from the Coastal Makran mud volcanoes, and ii) Na-HCO₃, pertaining to Pirgel, which also showed significantly high concentration of As, B and Li possibly fed by the rising CO₂-rich hydrothermal fluids. All the investigated waters were also marked by high B/Cl, Li/Cl and Na/Cl ratios and ¹⁸O-enriched and ²H-depleted water isotopes, suggesting a long-term fluid-mineral interaction and/or clay mineral dehydration. Mg-Li and Mg-K geothermometers data would suggest that formation of mud volcanic waters in onshore Makran proceeds at 84–165 °C, corresponding to 3–7 km depth, i.e. a deeper source with respect to that of mud volcanoes located in the Makran accretionary prisms of Pakistan.

The geochemical and isotopic features of the fluids carried out in this study should be considered as a prerequisite indication for possible occurrence of deep-seated hydrocarbon reservoir/s in Coastal Makran, though to be confirmed by geophysical and geological evidences. More detailed investigations at Pirgel, where a hydrothermal signature in the discharged waters and gases was recognized, should be carried out to evaluate the effective geothermal potential.

Acknowledgments

The authors would like to thank the Iran National Science Foundation (INSF), the Office of President, vice-Presidency for Science and Technology (project number 95850069) for partial financial support.

Appendix A. Supplementary data

Supplementary data to this article can be found online at <https://doi.org/10.1016/j.marpetgeo.2019.05.005>.

References

- Aghanabati, A., 1994. Geological Map of Khash, Scale: 1/250,000. Geological Survey and Mineral Exploration of Iran.
- Aloisi, G., Drews, M., Wallmann, K., Bohrmann, G., 2004. Fluid expulsion from the Dvurechenskii mud volcano (Black Sea) Part I. Fluid sources and relevance to Li, B, Sr, I and dissolved inorganic nitrogen cycles. *Earth Planet. Sci. Lett.* 225, 347–363.
- Arnórsson, S., Andrésdóttir, A., 1995. Processes controlling the distribution of boron and chlorine in natural waters in Iceland. *Geochem. Cosmochim. Acta* 59, 4125–4146.
- Ballentine, C.J., Burnard, P.G., 2002. Production, release and transport of noble gases in continental crust. In: In: Porcelli, D., Ballentine, C.J., Wieler, R. (Eds.), *Noble Gases in Geochemistry and Cosmochemistry*, vol. 47. *Rev. Mineral. Geochem.*, pp. 481–537.
- Bencini, A., 1985. Applicabilità del metodo dell'Azometina-H alla determinazione del boro nelle acque naturali. *Rendiconti della Soc. Ital. Mineral. Petrol.* 40, 311–316.
- Bernard, B.B., Brooks, J.M., Sackett, W.M., 1978. Light hydrocarbons in recent Texas continental shelf and slope sediments. *J. Geophys. Res.* 83, 4053–4061.
- Bhattacharya, P., Claesson, M., Bundschuh, J., Sracek, O., Fagerberg, J., Jacks, G., Martin, R.A., Storniolo, A., Thir, M., 2006. Distribution and mobility of arsenic in the Rio Dulce alluvial aquifers in Santiago del Estero Province, Argentina. *Sci. Total Environ.* 358, 97–120.
- Blinova, V.N., Ivanov, M.K., Böhrmann, G., 2003. Hydrocarbon gases in deposits from mud volcanoes in the Sorokin trough, north-eastern Black Sea. *Geo Mar. Lett.* 23 (3–4), 250–257.
- Brown, K.M., 1990. The nature and hydrological significance of mud diapirism and diatremes for accretionary systems. *J. Geophys. Res.* 95, 8969–8982.
- Bundschuh, J., Maity, J.P., 2015. Geothermal arsenic: occurrence, mobility and environmental implications. *Renew. Sustain. Energy Rev.* 42, 1214–1222.
- Chao, H.C., You, C.F., Wang, B.S., Chung, C.H., Huang, K.F., 2011. Boron isotopic composition of mud volcano fluids: implications for fluid migration in shallow subduction zones. *Earth Planet. Sci. Lett.* 305, 32–44.
- Chiodini, G., D'Alessandro, W., Parello, F., 1996. Geochemistry of gases and waters discharged by the mud volcanoes at Paterno, Mt. Etna (Italy). *Bull. Volcanol.* 58, 51–58.
- Ciotoli, G., Etiope, G., Marra, F., Florindo, F., Giraudi, C., Ruggiero, L., 2016. Tiber delta CO₂-CH₄ degassing: a possible hybrid, tectonically active Sediment-Hosted Geothermal System near Rome. *J. Geophys. Res. Solid Earths* 121.
- Cipriani, C., 1958a. Ricerche sui minerali costituenti le arenarie: 1) Sulla composizione mineralogica della frazione argillosa di alcune arenarie Macigno. *Atti della Società Toscana di Scienze Naturali* 65, 86–106.

- Cipriani, C., 1958b. Ricerche sui minerali costituenti le arenarie: 2) Sulla composizione mineralogica della frazione sabbiosa di alcune arenarie Macigno. *Atti Società Toscana di Scienze Naturali* 65, 165–220.
- Cipriani, C., Malesani, P.G., 1972. Composizione mineralogica delle frazioni pelitiche delle Formazioni del Macigno e Marnoso-Arenacea (Appennino settentrionale). *Mem. Ist. Geol. E. Min.* 29, 1–25.
- Colten-Bradley, V.A., 1987. Role of pressure in smectite dehydration—effects on geo-pressure and smectite-to-illite transformation. *AAPG Bull.* 71, 1414–1427.
- Dela Pierre, F., Martire, L., Natalicchio, M., Clari, P., Petrea, C., 2010. Authigenic carbonates in Upper Miocene sediments of the Tertiary Piedmont Basin (NW Italy): vestiges of an ancient gas hydrate stability zone? *Geol. Soc. Am. Bull.* 122, 994–1010.
- Delisle, G., von Rad, U., Andruleit, H., von Daniels, C.H., Tabrez, A.R., Inam, A., 2002. Active mud volcanoes on- and offshore eastern Makran, Pakistan. *J. Earth Sci.* 91, 93–110.
- Deville, E., Guerlais, S.H., Callec, Y., Griboulard, R., Huyghe, P., Lallemand, S., Mascle, A., Noble, M., Schmitz, J., 2006. Liquefied vs. stratified sediment mobilization processes: insight from the South of the Barbados accretionary prism. *Tectonophysics* 428, 33–47.
- Dia, A.N., Castrec-Rouelle, M., Boulégué, J., Comeau, P., 1999. Trinidad mud volcanoes: where do the expelled fluids come from? *Geochem. Cosmochim. Acta* 63, 1023–1038.
- Diaz-del-Rio, V., Somoza, L., Martínez-Frias, J., Mata, M.P., Delgado, A., Hernandez Molina, F.J., Lunar, R., Martín-Rubi, J.A., Maestro, A., Fernández-Puga, M.C., Leon, R., Liave, E., Medialdea, T., Vazquez, J.T., 2003. Vast fields of hydrocarbon derived carbonate chimneys related to the accretionary wedge/olistostrome of the Gulf of Cadiz. *Mar. Geol.* 195, 177–200.
- Dimitrov, L.I., 2002. Mud volcanoes—the most important pathway for degassing deeply buried sediments. *Earth Sci. Rev.* 59, 49–76.
- Dolati, A., 2010. Stratigraphy, Structural Geology and Low-Temperature Thermochronology across the Makran Accretionary Wedge in Iran. PhD thesis. geological institute of Swiss Federal, pp. 309.
- Dählmann, A., de Lange, G.J., 2003. Fluid-sediment interactions at Eastern Mediterranean mud volcanoes: a stable isotope study from ODP Leg 160. *Earth Planet. Sci. Lett.* 212, 377–391.
- Etiopie, G., Feyzullayev, A., Baci, C.L., Milkov, A.V., 2004. Methane emission from mud volcanoes in eastern Azerbaijan. *Geology* 32, 465–468.
- Etiopie, G., Feyzullayev, A., Baci, C.L., 2009. Terrestrial methane seeps and mud volcanoes: a global perspective of gas origin. *Mar. Pet. Geol.* 26, 333–344.
- Evans, W.C., White, L.D., Rap, P., 1998. Geochemistry of some gases in hydrothermal fluids from the southern Juan de Fuca ridge. *J. Geophys. Res.* 15, 305–313.
- Fontes, J.Ch., Matray, J.M., 1993. Geochemistry and origin of formation brines from the Paris Basin, France: 1. brines associated with Triassic salts. *Chem. Geol.* 109, 149–175.
- Fowler, S.R., White, R.S., Loudon, K.E., 1985. Sediment dewatering in the Makran accretionary prism. *Earth Planet. Sci. Lett.* 75, 427–438.
- Giammanco, S., Parello, F., Gambardella, B., Schifano, R., Pizzullo, S., Galante, G., 2007. Focused and diffuse effluents of CO₂ from mud volcanoes and mofettes south of Mt. Etna (Italy). *J. Volcanol. Geotherm. Res.* 165, 46–63.
- Giggenbach, W.F., 1988. Geothermal solute equilibria: derivation of Na-K-Mg-Ca geoindicators. *Geochem. Cosmochim. Acta* 52, 2749–2765.
- Grando, G., McClay, K., 2007. Morphotectonics domains and structural styles in the Makran accretionary prism, offshore Iran. *Sediment. Geol.* 196, 157–179.
- Haghipour, N., 2013. Active Deformation and Landscape Evolution of the Makran Accretionary Wedge (SE-Iran) New Constraints from Surface Exposure Dating of Fluvial Terraces. PhD thesis. ETH Zurich, pp. 165.
- Harms, J.C.C., Cappel, H.N., Francis, D.C., 1982. Geology and Petroleum Potential of Makran Coast, Pakistan. Offshore South East Asia Conference, Singapore.
- Harms, J.C., Cappel, H.N., Francis, D.C., 1984. The Makran coast of Pakistan: its stratigraphy and hydrocarbon potential. In: Haq, B.U., Milliman, J.D. (Eds.), *Marine Geology and Oceanography of the Arabian Sea and Coastal Pakistan*. Van Nostrand Reinhold, New York, pp. 3–26.
- Hensen, C., Wallmann, K., Schmidt, M., Ranero, C.R., Suess, E., 2004. Fluid expulsion related to mud extrusion off Costa Rica—a window to the subducting slab. *Geology* 32, 201–204.
- Hensen, Ch., Nuzzo, M., Hornibrook, E.R.C., Pinheiro, L.M., Bock, B., Magalhaes, V., Brückmann, W., 2007. Sources of mud volcano fluids in the Gulf of Cadiz-indication for hydrothermal imprint. *Geochem. Cosmochim. Acta* 71 (5), 1232–1248.
- Hensen, C., et al., 2015. Strike-slip faults mediate the rise of crustal-derived fluids and mud volcanism in the deep sea. *Geology* 43, 339–342.
- Hilton, D.R., Fischer, T.P., Marty, B., 2002. Noble gases and volatile recycling at subduction zones. *Rev. Mineral. Geochem.* 47 (1), 319–370.
- Himmler, T., Birgel, D., Bayon, G., Pape, Th., Ge, L., Bohrmann, G., Peckmann, J., 2015. Formation of seep carbonates along the Makran convergent margin, northern Arabian Sea and a molecular and isotopic approach to constrain the carbon isotopic composition of parent methane. *Chem. Geol.* 415, 102–117.
- Hoke, L., Hilton, D.R., Lamb, S.H., Hammerschmidt, K., Friedrichsen, H., 1994. ³He evidence for a wide zone of active mantle melting beneath the Central Andes. *Earth Planet. Sci. Lett.* 128, 341–355.
- Holford, S.P., Schofield, N., Jackson, C.A.L., Magee, C., Green, P.F., Duddy, I.R., 2013. Impacts of igneous intrusions on source and reservoir potential in prospective sedimentary basins along the Western Australian Continental Margin. In: Keep, M., Moss, S.J. (Eds.), *The Sedimentary Basins of Western Australia IV*. Proceedings of the Petroleum Exploration Society of Australia Symposium, Perth, WA.
- Hosseini-Barzai, M., Talbot, C.J., 2003. A tectonic pulse in the Makran accretionary prism recorded in Iranian coastal sediments. *J. Geol. Soc. Lond.* 160, 903–910.
- Hunt, J.M., 1996. *Petroleum Geochemistry and Geology*, second ed. Freeman, W.H., San Francisco, California, pp. 743.
- Inguaggiato, S., Rizzo, A.L., 2004. Dissolved helium isotope ratios in ground-waters: a new technique based on gas-water re-equilibration and its application to Stromboli volcanic system. *Appl. Geochem.* 19 (5), 665–673.
- James, R.H., Rudnicki, M.D., Palmer, M.R., 1999. The alkali element and boron geochemistry of the Escanaba Trough sediment-hosted hydrothermal system. *Earth Planet. Sci. Lett.* 171, 157–169.
- Kastner, M., Elderfield, H., Martin, J.B., 1991. Fluids in convergent margins: what do we know about their composition, origin, role in diagenesis and importance for oceanic chemical fluxes. *Phil. Trans. Roy. Soc. Lond.* A335, 243–259.
- Khan, M.A., Raza, H.A., Alam, S., 1991. Petroleum geology of the Makran region; implications for hydrocarbon occurrence in cool basins. *J. Pet. Geol.* 14 (1), 5–18.
- Kharaka, Y.K., Mariner, R.H., 1989. Chemical geothermometers and their application to formation waters from sedimentary basins. In: Nancy, N., McCulloh, D., Thane, H. (Eds.), *Thermal History of Sedimentary Basins, Methods and Case Histories*. Springer, New York, pp. 99–117.
- Kharaka, Y.K., Hanor, J.S., 2004. Deep fluids in the continents: 1. sedimentary basins. In: In: Drever, J.L., Holland, H.D., Turekian, K.K., Exec (Eds.), *Treatise on Geochemistry*, vol. 5. pp. 499–540.
- Kim, M.J., Nriagu, J., Haack, S., 2000. Carbonate ions and arsenic dissolution by groundwater. *Environ. Sci. Technol.* 34, 3094–3100.
- Kim, M.J., Nriagu, J., Haack, S., 2003. Arsenic behavior in newly drilled wells. *Chemosphere* 52, 623–633.
- Kopf, A., Klaeschen, D., Mascle, J., 2001. Extreme efficiency of mud volcanism in dewatering accretionary prisms. *Earth Planet. Sci. Lett.* 189, 295–313.
- Kopf, A., Deyhle, A., 2002. Back to the roots: boron geochemistry of mud volcanoes and its implications for mobilization depth and global B cycling. *Chem. Geol.* 192, 195–210.
- Kopf, A.J., 2002. Significance of mud volcanism. *Rev. Geophys.* 40 (2), 1–52.
- Kopp, C., Fruehn, J., Flueh, E.R., Reicher, C., Kukowski, N., Bialas, J., Klaeschen, D., 2000. Structure of the Makran subduction zone from wide angle and reflection seismic data. *Tectonophysics* 329, 171–191.
- Lavrushin, V.Yu., Dubinina, E.O., Avdeenko, A.S., 2005. Isotopic composition of oxygen and hydrogen in mud volcanic waters from Taman (Russia) and Kakhketia (Eastern Georgia). *Lithol. Miner. Resour.* 2, 123–137.
- Liang, H., Chen, X., Wang, Ch., Zhao, D., Weissert, H., 2016. Methane-derived authigenic carbonates of mid-Cretaceous age in southern Tibet: types of carbonate concretions, carbon sources, and formation processes. *J. Asian Earth Sci.* 115, 153–169.
- López, D.L., Bunschuh, J., Birkle, P., Armenta, M.A., Cumbal, L., Sracek, O., Cornejo, L., Ormachea, M., 2012. Arsenic in volcanic geothermal fluids of Latin America. *Sci. Total Environ.* 429, 57–75.
- Mamyrin, B.A., Tolstikhin, I.N., 1984. He isotopes in nature. *Dev. Geochem.* 3, 274.
- Marty, B., Jambon, A., Sano, Y., 1989. Helium isotopes and CO₂ in volcanic gases of Japan. *Chem. Geol.* 76, 25–40.
- Masson, B., 1966. *Principles of Geochemistry*, third ed. Wiley, NewYork.
- Mazzini, A., Svensen, H., Planke, S., Guliyev, I., Akhmanov, G.G., Fallik, T., Banks, D., 2009. When mud volcanoes sleep: insight from seep geochemistry at the Dashgil mud volcano, Azerbaijan. *Mar. Pet. Geol.* 26, 1704–1715.
- Mazzini, A., Svensen, H., Etiopie, G., Onderdonk, N., Banks, D., 2011. Fluid origin, gas fluxes and plumbing system in the sediment-hosted Salton Sea Geothermal System (California, USA). *J. Volcanol. Geotherm. Res.* 205, 67–83.
- Mazzini, A., Etiopie, G., 2017. Mud volcanism: an updated review. *Earth Sci. Rev.* 168, 81–112.
- Mazzini, A., Scholz, F., Svensen, H.H., Hensen, Ch., Hadi, S., 2017. The geochemistry and origin of the hydrothermal water erupted at Lusi, Indonesia. *Mar. Pet. Geol.* 1–15.
- McCall, G.J.H., 2002. A summary of the geology of the Iranian Makran. In: Clift Peter, D., Kroon, D., Gaedicke, C., Craig, J. (Eds.), *The Tectonic and Climatic Evolution of the Arabian Sea Region*. the Geological Society of London. Special Publications 195, pp. 1–5.
- Milkov, A.V., 2000. Worldwide distribution of submarine mud volcanoes and associated gas hydrates. *Mar. Geol.* 167, 29–42.
- Milkov, A.V., Sassen, R., Apanasovich, T.V., Dadashev, F.G., 2003. Global gas flux from mud volcanoes: a significant source of fossil methane in the atmosphere and the ocean. *Geophys. Res. Lett.* 30, 1037.
- Milkov, A.V., 2005. Global distribution of mud volcanoes and their significance in petroleum exploration, as a source of methane in the atmosphere and hydrosphere, and as geohazard. In: In: Martinelli, G., Panahi, B. (Eds.), *Mud Volcanoes: Geodynamics and Seismicity*. Nato. Sci. Sv. Iv. Ear. vol. 51. pp. 29–34.
- Minissale, A., Magro, G., Martinelli, G., Vaselli, O., Tassi, G.F., 2000. Fluid geochemical transect in the Northern Apennines (central-northern Italy): fluid genesis and migration and tectonic implications. *Tectonophysics* 319, 199–222.
- Miri, M., Rezaie, M., Khaksefidi, M., Khajeh Dad, Gh.H., 2014. Saravan earthquake, a case study. In: The 9th Symposium on Advances in Science and Technology (9thSASTech), Mashhad, Iran (in Persian).
- Moore, J.C., Vrolijk, P., 1992. Fluids in accretionary prisms. *Rev. Geophys.* 30, 113–135.
- Motyka, R., Nye, C., Turner, D., Liss, S., 1993. The geyser Bight geothermal area, Umnak Island, Alaska. *Geothermics* 22, 301–327.
- Naehr, T.H., Eichhubl, P., Orphan, V.J., Hovland, M., Paull, C.K., Ussler III, M., Lorenson, T.D., Greene, H.G., 2007. Authigenic carbonate formation at hydrocarbon seeps in continental margin sediments: a comparative study. *Deep-Sea Res. Pt. II* 54, 1268–1291.
- Negaresh, H., khosravi, M., 2008. The geomorphic and morphometric characteristics of Napag mud volcano in the south eastern of Iran. *J. Hum. Isfahan Univ.* 30, 51–68.
- Oppo, D., Capozzi, R., Nigarov, A., Esenov, P., 2014. Mud volcanism and fluid geochemistry in the Cheleken peninsula, western Turkmenistan. *Mar. Pet. Geol.* 57, 122–134.
- Oremland, R.S., Miller, L.G., Whiticar, M.J., 1987. Sources and flux of natural gases from

- Mono Lake, California. *Geochim. Cosmochim. Acta* 51, 2915–2929.
- Orpin, A.R., 1997. Dolomite chimneys as possible evidence of coastal fluid expulsion, uppermost Otago continental slope, southern New Zealand. *Mar. Geol.* 138, 51–67.
- Page, W.D., Alt, J.N., Cluff, L.S., Plafker, G., 1979. Evidence for the recurrence of large magnitude earthquakes along the Makran coast of Iran and Pakistan. *Tectonophysics* 52 (1–4), 533–547.
- Paikaray, S., 2012. Environmental hazards of arsenic associated with black shales: a review on geochemistry, enrichment and leaching mechanism. *Rev. Environ. Sci. Biotechnol.* 11, 289–303.
- Platt, J.P., Leggett, J.K., Young, J., Raza, H., Alam, S., 1985. Large-scale sediment underplating in the Makran accretionary prism, south-west Pakistan. *Geology* 13, 507–511.
- Poreda, R., Craig, H., 1989. Helium isotopes in circum-Pacific volcanic arcs. *Nature* 338, 473–478.
- Prinzhofer, A., Deville, E., 2013. Origins of hydrocarbon gas seeping out from offshore mud volcanoes in the Nile delta. *Tectonophysics* 591, 52–61.
- Quigley, T.M., MacKenzie, A.S., 1988. The temperatures of oil and gas formation in the sub-surface. *Nature* 333, 549–552.
- Ray, J.S., Kumar, A., Sudheer, A.K., Deshpande, R.D., Rao, D.K., Patil, D.J., Awasthi, N., Bhutani, R., Bhushan, R., Dayal, A.M., 2013. Origin of gases and water in mud volcanoes of Andaman accretionary prism: implications for fluid migration in forearcs. *Chem. Geol.* 347, 102–113.
- Reyss, J.L., Pirazzoli, P.A., Haghipour, A., Hatté, C., Fontugne, M., 1999. Quaternary marine terraces and tectonic uplift rates on the south coast of Iran. In: Stewart, I.S., Vita-Finzi, C. (Eds.), *Coastal Tectonics. Special Publication 146*. Geological Society, London, pp. 225–237.
- Rice, D.D., Claypool, G.E., 1981. Generation, accumulation and resource potential of biogenic gas. *AAPG Bull.* 65 (1), 5–25.
- Rittenhouse, G., 1967. Bromine in oil-field waters and its use in determining possibilities of origin of these waters. *AAPG Bull.* 51, 2430–2440.
- Sahandi, M.R., 1996. Geological Map of Iranshahr, Scale: 1/250000. Geological Survey and Mineral Exploration of Iran.
- Sain, K., Minshull, T.A., Singh, S.C., Hobbs, R.W., 2000. Evidence for a thick free gas layer beneath the bottom simulating reflector in the Makran accretionary prism. *Mar. Geol.* 164, 3–12.
- Saket, A., Fatemi Aghda, S.M., Khadivi, Sh., 2005. Study of seismic parameters of Bam and Zaran earthquake with emphasis on aftershocks. In: *The 9th Symposium of Iran Geology Society (In Persian)*, pp. 161–169.
- Sano, Y., Marty, B., 1995. Origin of carbon in fumarolic gas from island arcs. *Chem. Geol.* 119, 265–274.
- Sano, Y., Williams, S.N., 1996. Fluxes of mantle and subducted carbon along convergent plate boundaries. *Geophys. Res. Lett.* 23, 2749–2752.
- Schlüter, H.U., Prexl, A., Gaedicke, Ch., Roeser, H., Reichert, Ch., Meyer, H., von Daniels, C., 2002. The Makran accretionary wedge: sediment thicknesses and ages and the origin of mud volcanoes. *Mar. Geol.* 3087, 1–14.
- Schoell, M., 1980. The hydrogen and carbon isotopic composition of methane from natural gases of various origins. *Geochem. Cosmochim. Acta* 44, 649–661.
- Schoell, M., 1988. Multiple origins of methane in the Earth. *Chem. Geol.* 71, 1–10.
- Scholz, F., Hensen, C., De Lange, G.J., Haeckel, M., Liebetrau, V., Meixner, A., Reitz, A., Romer, R.L., 2010. Lithium isotope geochemistry of marine pore waters—insights from cold seep fluids. *Geochem. Cosmochim. Acta* 74, 3459–3475.
- Shakeri, A., Moore, F., Kompani-zare, M., 2008. Geochemistry of the thermal springs of Mount Taftan, southeastern Iran. *J. Volcanol. Geotherm. Res.* 178, 829–836.
- Shakeri, A., Ghoreyshinia, S.K., Mehrabi, B., 2014. Surface and groundwater quality in Taftan geothermal field, SE Iran. *Water Qual. Expo. Health* 7 (2).
- Shakirov, R., Obzhairov, A., Suess, E., Salyuk, A., Biebow, N., 2004. Mud volcanoes and gas vents in the Okhotsk Sea area. *Geo Mar. Lett.* 24, 140–149.
- Shamsi, A., Kazemi, G.A., 2014. A review of research dealing with isotope hydrology in Iran and the first Iranian meteoric water line. *Geopersia* 4 (1), 73–86.
- Simmons, S.F., Brown, K.L., Browne, P.R., Rowland, J.V., 2016. Gold and silver resources in Taupo Volcanic Zone geothermal systems. *Geothermics* 59, 205–214.
- Stöcklin, J., 1968. Structural history and tectonics of Iran: a review. *AAPG Bull.* 52, 1229–1258.
- Takai, K., Nakamura, K., Toki, T., Tsunogai, U., Miyazaki, M., Miyazaki, J., Hirayama, H., Nakagawa, S., Nunoura, T., Horikosh, K., 2008. Cell proliferation at 122 degrees C and isotopically heavy CH₄ production by a hyperthermophilic methanogen under high-pressure cultivation. *Proc. Natl. Acad. Sci. U.S.A.* 105, 10949–10954.
- Tassi, F., Bonini, M., Montegrossi, G., Capecchiacci, F., Capaccioni, B., Vaselli, O., 2012. Origin of light hydrocarbons in gases from mud volcanoes and CH₄-rich emissions. *Chem. Geol.* 294–295, 113–126.
- Teichert, B.M.A., Torres, M.E., Bohrmann, G., Eisenhauer, A., 2005. Fluid sources, fluid pathways and diagenetic reactions across an accretionary prism revealed by Sr and B geochemistry. *Earth Planet. Sci. Lett.* 239 (1–2), 106–121.
- Tirral, R., Bell, I.R., Griffis, R.J., Camp, V.E., 1983. The Sistan suture zone of eastern Iran. *Geol. Soc. Am. Bull.* 94 (1), 134–150.
- Tissot, B.P., Welte, D.H., 1978. *Petroleum Formation and Occurrence*. Springer-Verlag Berlin Heidelberg, New York Tokyo, pp. 699.
- Vaselli, O., Tassi, F., Montegrossi, G., Capaccioni, B., Giannini, L., 2006. Sampling and analysis of volcanic gases. *Acta Volcanol.* 18, 65–76.
- Verma, S.P., Santoyo, E., 1997. New improved equations for Na/K, Na/Li and SiO₂ geothermometers by outlier detection and rejection. *J. Volcanol. Geotherm. Res.* 79, 9–23.
- Wan, Z., Shi, Q., Guo, F., Zhong, Y., Xia, B., 2013. Gases in Southern Junggar Basin mud volcanoes: chemical composition, stable carbon isotopes, and gas origin. *J. Nat. Gas Sci. Eng.* 14, 108–115.
- Webster, J.G., Nordstrom, D.K., 2003. Geothermal arsenic: the sources, transport and fate of arsenic in geothermal systems. In: Welch, A.H., Stollenwerk, K.G. (Eds.), *Arsenic in Groundwater: Geochemistry and Occurrence*. Kluwer Academic Publishers, Boston, pp. 101–125.
- White, R.S., 1979. Gas hydrate layers trapping free gas in the Gulf of Oman. *Earth Planet. Sci. Lett.* 42 (1), 114–120.
- Whiticar, M.J., Faber, E., Schoell, M., 1986. Biogenic methane formation in marine and fresh water environments: CO₂ reduction vs. acetate fermentation—isotope evidence. *Geochem. Cosmochim. Acta* 50, 693–709.
- Whiticar, M.J., 1999. Carbon and hydrogen isotope systematics of bacterial formation and oxidation of methane. *Chem. Geol.* 161, 291–314.
- Williams, L.B., Hervig, R.L., Holloway, J.R., Hutcheon, I., 2001. Boron isotope geochemistry during diagenesis, part I. experimental determination of fractionation during illitization of smectite. *Geochem. Cosmochim. Acta* 65, 1769–1782.
- Wrage, J., Tardani, D., Reich, M., Daniele, L., Arancibia, G., Cembrano, J., Sánchez-Alfaro, P., Morata, D., Pérez-Moreno, R., 2017. Geochemistry of thermal waters in the Southern Volcanic Zone, Chile—Implications for structural controls on geothermal fluid composition. *Chem. Geol.* 466, 545–561.
- Wycherley, H., Fleet, A., Shaw, H., 1999. Some observations on the origins of large volumes of carbon dioxide accumulations in sedimentary basins. *Mar. Pet. Geol.* 16, 489–494.
- Yang, T.F., Yeh, G.H., Fu, C.C., Wang, C.C., Lan, T.F., Lee, H.F., Chen, C.H., Walia, V., Sung, Q.C., 2004. Composition and exhalation flux of gases from mud volcanoes in Taiwan. *Environ. Geol.* 46, 1003–1011.
- You, C.F., Spivack, A.J., Smith, J.H., Gieskes, J.M., 1993. Mobilization of boron in convergent margins: implications for the boron geochemical cycle. *Geology* 21, 207–221.
- You, C.F., Castillo, P.R., Gieskes, J.M., Chan, L.H., Spivack, A.J., 1996. Trace element behavior in hydrothermal experiments: implications for fluid processes at shallow depths in subduction zones. *Earth Planet. Sci. Lett.* 140, 41–52.
- You, C.F., Gieskes, J.M., Leec, T., Yuic, T.F., Chenc, H.W., 2004. Geochemistry of mud volcano fluids in the Taiwan accretionary prism. *Appl. Geochem.* 19, 695–707.
- Younger, P.L., 2007. *Groundwater in the Environment: an Introduction*. Blackwell Publishing, USA.